AIR-OIL MIST LUBRICATION OF SMALL BORE BALL BEARINGS AT HIGH SPEEDS

by

Francis Douglas Pinckney

Thesis submitted to the Faculty of the
Virginia Polytechnic Institute and State University
in partial fulfillment of the requirements for the degree of

MASTER OF SCIENCE

in

Mechanical Engineering

APPROVED:

W. F. O'Brien, Chairman

C. E. Knight

H. H. Mabie

August, 1985

Blacksburg, Virginia

AIR-OIL MIST LUBRICATION OF SMALL BORE BALL BEARINGS AT HIGH SPEEDS

by

Francis Douglas Pinckney

ABSTRACT

Deep groove and angular contact 25 and 30 mm bore ball bearings were tested to high speeds using air-oil mist lubrication. Test conditions included cooling air flow rates of 1.5, 3.0, and 6.0 scfm (0.05, 0.10, and 0.20 kg/min), thrust loads of 50, 75, and 100 lb (222, 334, and 445 N), and a constant radial load of 25 lb (111 N). Steady-state bearing outer race temperature was recorded at various speeds under each set of test conditions.

Maximum DN values of 1.9×10^6, 1.5×10^6, 1.4×10^6, and 1.26×10^6 were achieved on the 30 mm deep groove, the 25 mm deep groove, the 25 mm angular contact, and the 30 mm angular contact bearings, respectively. Tests were usually terminated when the stabilized outer race temperature reached approximately 200°F (366 K) although the 30 mm deep groove bearing was operated to 240°F (389 K).

A cooling air flow rate of 1.5 scfm (0.05 kg/min) was judged not adequate for high speed bearing operation under the tested conditions.

An outer-race temperature prediction equation, based on a regression analysis of the test results, is presented for each test bearing.

ACKNOWLEDGMENTS

I would like to express my gratitude for the financial support from Industrial Drives Division of Kollmorgen Corporation during this project.

I would also like to thank my committee, Dr. W. F. O'Brien, Dr. C. E. Knight, and Dr. H. H. Mabie for their assistance and patience on this project.

I am especially grateful to my friend, Philip Gatz, for the statistical analysis assistance provided on such short notice.

I am also grateful to my supervisor, Mr. Henry McFadden, for his patience with my sometimes unusual working hours as I finished this thesis.

Finally, I would especially like to thank my wife, Margaret, for her patience, encouragement, and loving support during my studies at Virginia Tech.

TABLE OF CONTENTS

	Page
ABSTRACT	
ACKNOWLEDGMENTS	iii
LIST OF FIGURES	v
LIST OF TABLES	viii
I. INTRODUCTION	1
II. LITERATURE REVIEW	7
III. BEARING TEST RIG AND EXPERIMENTAL PROCEDURE	13
IV. RESULTS	25
V. ANALYSIS OF RESULTS	58
VI. DISCUSSION OF RESULTS	68
VII. CONCLUSIONS	75
VIII. RECOMMENDATIONS	76
REFERENCES	78
APPENDIX A: Test Rig Campbell Diagrams	80
APPENDIX B: Regression Analysis Statistics	87
VITA	90

LIST OF FIGURES

Fig. No.		Page
1.	Typical Oil Jet and Under-Race Lubrication Methods . . .	4
2.	Theoretical and Experimental Heat Generation Rates from the SKF Study (11)	11
3.	High Speed Bearing Test Rig	14
4.	Test Results for the 25mm Deep Groove Bearing with a 1.5 scfm Air Flow	31
5.	Test Results for the 25mm Deep Groove Bearing with a 3.0 scfm Air Flow	32
6.	Test Results for the 25mm Deep Groove Bearing with a 6.0 scfm Air Flow	33
7.	Test Results for the 25mm Deep Groove Bearing with a 50 lb Thrust Load	34
8.	Test Results for the 25mm Deep Groove Bearing with a 75 lb Thrust Load	35
9.	Test Results for the 25mm Deep Groove Bearing with a 100 lb Thrust Load	36
10.	Test Results for the 25mm Angular Contact Bearing with a 1.5 scfm Air Flow	37
11.	Test Results for the 25mm Angular Contact Bearing with a 3.0 scfm Air Flow	38
12.	Test Results for the 25mm Angular Contact Bearing with a 6.0 scfm Air Flow	39
13.	Test Results for the 25mm Angular Contact Bearing with a 50 lb Thrust Load	40
14.	Test Results for the 25mm Angular Contact Bearing with a 75 lb Thrust Load	41
15.	Test Results for the 25mm Angular Contact Bearing with a 100 lb Thrust Load	42
16.	Test Results for the 30mm Deep Groove Bearing with a 1.5 scfm Air Flow	43

LIST OF FIGURES (cont.)

Fig. No.		Page
17.	Test Results for the 30mm Deep Groove Bearing with a 3.0 scfm Air Flow	44
18.	Test Results for the 30mm Deep Groove Bearing with a 6.0 scfm Air Flow	45
19.	Test Results for the 30mm Deep Groove Bearing with a 50 lb Thrust Load	46
20.	Test Results for the 30 mm Deep Groove Bearing with a 75 lb Thrust Load	47
21.	Test Results for the 30mm Deep Groove Bearing with a 100 lb Thrust Load	48
22.	Test Results for the 30mm Angular Contact Bearing with a 1.5 scfm Air Flow	49
23.	Test Results for the 30mm Angular Contact Bearing with a 3.0 scfm Air Flow	50
24.	Test Results for the 30mm Angular Contact Bearing with a 6.0 scfm Air Flow	51
25.	Test Results for the 30mm Angular Contact Bearing with a 50 lb Thrust Load	52
26.	Test Results for the 30mm Angular Contact Bearing with a 75 lb Thrust Load	53
27.	Test Results for the 30mm Angular Contact Bearing with a 100 lb Thrust Load	54
28.	Test Results for the 17mm Deep Groove Support Bearing with a 71 lb Thrust Load and 13 lb Radial Load	55
29.	Test Results for the 17mm Deep Groove Support Bearing with a 96 lb Thrust Load and 13 lb Radial Load	56
30.	Test Results for the 17mm Deep Groove Support Bearing with a 121 lb Thrust Load and 13 lb Radial Load	57
31.	Test Bearing Temperature Prediction Equations	63
32.	Comparison of Correlation Prediction and Actual Results for the 25mm Deep Groove Bearing	64

LIST OF FIGURES (cont.)

Fig. No.		Page
33.	Comparison of Correlation Prediction and Actual Results for the 25mm Angular Contact Bearing	65
34.	Comparison of Correlation Prediction and Actual Results for the 30mm Deep Groove Bearing	66
35.	Comparison of Correlation Prediction and Actual Results for the 30mm Angular Contact Bearing	67
A-1	Campbell Diagram for the Drive Turbine	81
A-2	Campbell Diagram for the Bearing Test Unit with a 50 lb Test Bearing Thrust Load	82
A-3	Campbell Diagram for the Bearing Test Unit with a 75 lb Test Bearing Thrust Load	83
A-4	Campbell Diagram for the Bearing Test Unit with a 100 lb Test Bearing Thrust Load	84
A-5	Bearing Test Unit Mode Shape	85
A-6	Bearing Test Unit Mode Shape	86

LIST OF TABLES

Table		Page
1.	Flowmeter Scale Fctors for Various Pressures	18
2.	Test and Support Bearing Specifications	20
3.	Specifications of Lubricant Used During Testing	22
4.	Summary of Maximum Test Bearing Speeds Achieved	29
5.	Predicted Test Bearing Speeds for a 200°F Outer Race Temperature	72
B-1.	Regression Analysis Statistics for the 25 mm Bearings	88
B-2.	Regression Analysis Statistics for the 30 mm Bearings	89

I. INTRODUCTION

High speed ball bearings are used in many applications such as gas turbines, superchargers, and machine tool spindles where increasingly higher speeds are being required to meet performance objectives. Aircraft gas turbine engine development, in particular, has spurred much of the recent research in high speed bearings [1]*. This research, along with continued work by precision bearing manufacturers, has resulted in the availability of bearings with improved speed ratings. Still, bearing catalog speed ratings are generally conservative estimates based on past experiences for normal applications [2]. Adequate lubrication and cooling are critical factors in meeting or exceeding the catalog speed limit for properly installed precision ball bearings.

In any rolling element bearing, high speed operation results in increased centrifugal loading of the rolling elements and the outer race, and higher heat generation due to friction and lubricant churning. Increased centrifugal loading results in decreased fatigue life, but excessive heat generation can result in rapid failure due to lubricant film loss and resulting metal to metal contact. Severe wear and binding can result at the ball-cage and cage-race sliding contact interfaces. Excessive heat can also result in loss of bearing internal clearances, causing seizure. For these reasons, achieving a stabilized operating temperature is critical for successful high speed operation.

Before reviewing bearing lubrication and cooling methods used for

---

*References are denoted by numbers in brackets and are listed after the Recommendations section.

high speed applications, two factors used in rating ball bearings for high speed use should be introduced. The DN factor is most commonly used for evaluating bearings for high speed operation. The bearing DN is computed simply by multiplying the bearing bore in millimeters by the maximum speed in RPM. Although uncommon, some sources [3] use the pitch diameter (usually taken as one half the sum of the bore and the outside diameter) rather than the bore in computing DN. DN factors can be misleading when comparing the performance of bearings of differing bores. Zaretsky of the NASA Lewis Research Center points out that "for a given DN value, centrifugal effects are more severe with small bearings since centrifugal forces vary with DN^2 [4]. Comparison using DN values should therefore be limited to a narrow range of bearing sizes.

The TAC factor, although not in widespread use, is recommended by Bailey and Galbato of TRW Bearings Division [2] as a better indication of bearing high speed capability. They note that DN factors consider neither differences in bearing cross sections nor contact angles for bearings of the same bore. "Heavy" series ball bearings usually have larger race cross sections, larger rolling elements, and a resulting larger pitch diameter, all contributing to reduce speed capability. The TAC factor, τ, has been defined as

$$\tau = \frac{D_p N^3 d^3}{\cos^3 \beta}$$

where D_p is the pitch diameter in mm, N is the speed in revolutions per second, d is the ball diameter in inches, and β is the nominal contact angle in degrees. While the TAC factor is not as convenient to use, it

does include far more effects than the DN factor and can be used to advantage in many applications. The practical limiting TAC factor for precision ball bearings is about 31×10^8. This corresponds to a DN of about 2.5×10^6 for a typical "light" series bearing with a 25 or 30 mm bore.

Lubrication methods for ball bearings include grease, oil bath, wick, air-oil mist, oil jet and under-race lubrication. High speed applications are generally limited to air-oil mist, oil jet, and under-race lubrication to provide adequate cooling as well as lubrication. In oil jet systems a high velocity oil jet directed through a nozzle impinges on the inner race and ball contact area to provide both lubrication and a cooling effect. In under-race or through-the-race methods, oil flows through a hollow shaft and is directed outward through passages in the shaft through radial holes to the bearing inner race providing direct lubrication and cooling of the inner race. Figure 1 shows typical oil jet and under-race configurations [5]. Generally, higher DN values can be reached with under-race lubrication rather than with oil jet, since better cooling and lubrication of the inner race can be achieved. The inner race is typically more difficult to lubricate since the oil is centrifuged to the outer portion of the bearing.

Under-race lubrication is not commonly used in small bore ball bearings (40 mm and under) due to the difficulty in machining the grooves and radial holes required in the limited space available [4,1]. This method also requires the aquisition of special bearings with properly located radial holes through the inner race. Oil jet lubrication is much simpler and is in common use on aircraft gas tur-

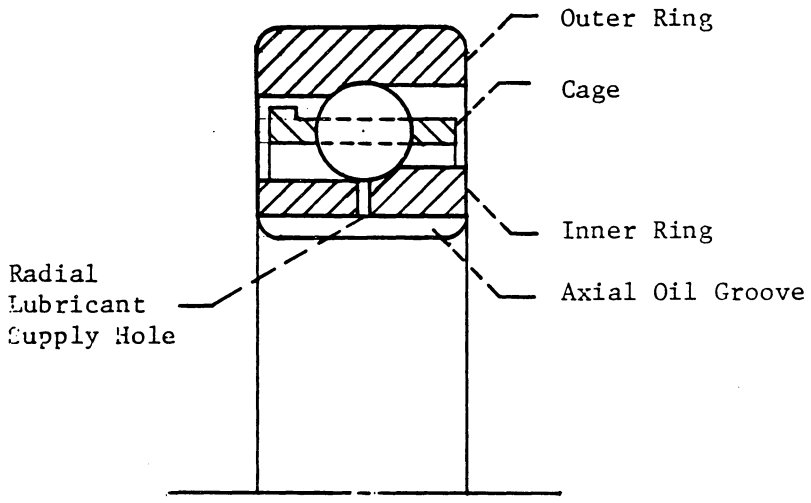

(a) Inner-Ring Lubricated

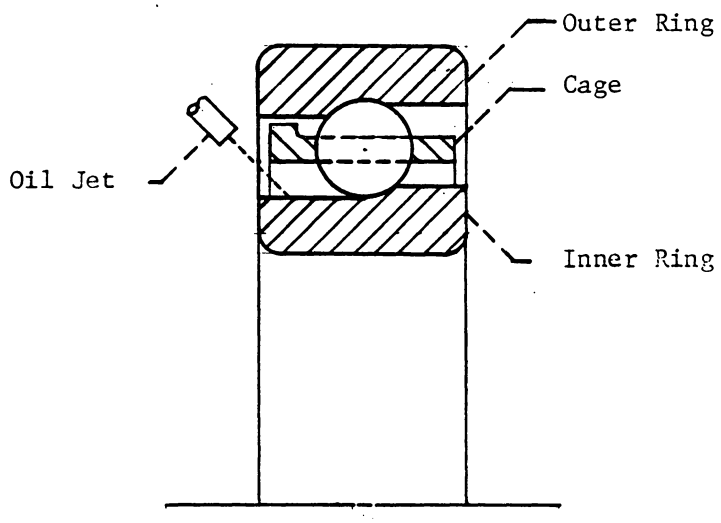

(b) Jet Lubricated

Fig. 1 Typical Oil Jet and Under-Race Lubrication Methods

bines. Both oil jet and under-race lubrication require oil recovery, recirculation, cooling and filtering and thus may not be practical or cost effective in many applications.

Air-oil mist systems use an oil mist generator to entrain minute oil particles in an air jet. The air-oil mist is then directed through a reclassifying nozzle at the bearing inner race, as in the oil jet method. The reclassifying nozzle is used to "condense" the minute oil particles into oil drops that provide a good wetting action on the bearing surfaces. Cooling comes primarily from the air stream as the oil flowrate is generally very low. Although air cooling is not as effective as oil cooling in the oil jet and under-race systems, the reduced quantity of oil results in less heat generation due to churning. Air-oil mist systems have the disadvantage of generally being a total oil loss system, but again, oil flow rates are small.

Air-oil mist lubricated bearings are generally limited to lower DN values than oil jet or under-race lubrication methods. Still, DN values in excess of bearing catalog limits can be achieved if adequate air and oil flow rates are established. While air-oil mist systems are commonly used in industrial applications, quantitative data on air and oil flow requirements for high speed operation are not readily available. A possible reason for this is that the rather general methods for estimating required air-oil mist flow rates put forth by the air-oil mist equiment manufacturers [6] are adequate only for operating speeds below catalog ratings. Further, for very high DN applications such as aircraft gas turbines, air-oil mist is generally ruled out as inadequate and oil jet systems are very convenient. Thus the bulk of the

quantitative data on lubrication of ball bearings at high speeds pertains to oil jet systems.

The purpose of the present investigation was to experimentally determine the air-oil mist flow requirements to achieve a stabilized operating temperature at high speeds for selected small bore ball bearings. Specifically, 25 and 30 mm light series deep groove and angular contact ball bearings were tested under three air-oil mist flow rates and three load conditions, resulting in 36 controlled test runs. Although not primary test bearings, data were also taken on two 17 mm deep groove test shaft support bearings. Outer race temperature was monitored on all bearings during the test runs. A single air-oil mist nozzle per bearing was used for all tests. Although lubrication can greatly affect fatigue life of ball bearings [1,7], no fatigue life tests were run in this investigation.

II. LITERATURE REVIEW

Research in lubrication of high speed ball bearings has been spurred by aircraft gas turbine engine developments. Much of the research has therefore been directed in the area of oil jet and under-race lubrication since these methods are readily adaptable to gas turbine engines. It is informative to review some of these efforts, although much of the data is not directly applicable to air-oil mist lubrication.

The NASA Lewis Research Center has done a number of tests on jet and under-race-lubricated small bore angular contact ball bearings. These tests were performed on a bearing test rig developed under contract for NASA. The significant features of this rig included an air turbine drive capable of 100,000 RPM, variable thrust and radial loading to 1000 pounds (4448 N) and adaptability to bearings having a 25 to 30 mm bore [8].

Schuller, Pinel, and Signer of NASA [9] tested 35 mm angular contact bearings to 2.5 x 10^6 DN (72,000 RPM) with jet lubrication using a synthetic lubricant with an inlet temperature of 250°F (394 K). Tests were run with thrust loads of 150 and 300 pounds (667 and 1334 N) and with combined thrust and radial loads of 150 and 50 pounds (667 and 222 N), respectively. Lubricant flow rates ranged from 0.02 to 0.5 gal/min (76 to 1894 cm^3/min) and represent oil flows two to three orders of magnitude larger than those used in air-oil mist systems. A maximum bearing outer ring temperature of 418°F (487 K) and inner ring temperature of 390°F (472 K) occurred with the 300 pound (1334 N) thrust load. Surprisingly, the inner ring temperature was generally lower than the outer ring temperature throughout the test. This was assumed to be

due to the oil jet being directed primarily at the inner race.

Similar results were obtained in another NASA test in which under-race lubrication was used on a 35 mm angular contact bearing [5]. The lower inner ring temperature was again assumed to be due to the large quantity of oil being directed primarily at the inner ring through the under-race grooves and holes (see Fig. 1). The under-race lubrication did result in lower inner ring temperatures and higher outer ring temperatures than the jet lubricated bearing.

A study on jet lubrication with 30 mm deep groove and angular contact bearings by the Japanese National Aerospace Laboratory preceded the NASA work above [10]. This report laid the groundwork for the NASA work in terms of optimum bearing characteristics, oil jet velocity, and nozzle position for high speed jet lubricated bearings. A petroleum-based turbine oil at 86°F (303 K) inlet temperature, oil flows ranging from approximately 0.07 to 0.9 gal/min (0.22 to 3.0 kg/min) and a 110 pound (490 N) thrust load were used for most of the tests. This report and later NASA work indicates that bearing cage design is often the limiting factor for high speeds.

In the Japanese study, inner and outer race guided cages were tested in both the deep groove and angular contact bearings. An amazing 3.0×10^6 DN (100,000 RPM) was achieved on the angular contact bearing with the outer ring guided cage at oil flows as low as 0.2 gal/min (0.72 kg/min). The maximum outer race temperature varied from 352°F (451 K) to 241°F (389 K) for oil flows from 0.07 to 0.9 gal/min (0.72 to 3 kg/min). Prolonged operation at these temperatures is questionable using a petroleum-based lubricant.

In other tests, 2.8×10^6 DN was achieved with the deep groove outer race guided cage bearing, and 2.3×10^6 DN and 1.6×10^6 DN were achieved on the angular contact and deep groove bearings respectively, with inner race guided cages. In these cases, the maximum speed was limited by insufficient lubrication to the critical sliding contact areas at the cage-race and cage-ball interfaces. Excessive friction, binding, and resulting failure occur with insufficient lubrication to these critical areas. The cage configuration of the angular contact outer race guided cage bearing resulted in the best lubrication of the critical sliding contact areas.

In a brief report by the Japanese National Aerospace Laboratory (for which, unfortunately, no complete technical translation was available) 30 mm angular contact bearings were tested with both air-oil mist and oil jet lubrication [11]. A thrust load of 110 pounds (490 N) and a petroleum-based oil were again used in these tests. A top speed of 2.16×10^6 DN (72,000 RPM) was achieved with air-oil mist but a tremendous air flow of 90 scfm (3 kg/min) and an oil flow of 1.0×10^{-3} gal/min (4 mℓ/min) were required. The oil jet-lubricated bearing was operated to 3.27×10^6 DN (109,000 RPM) with oil flows above 0.6 gal/min (2 kg/min). A review of the figures published in this report showed that additional lower air-oil mist flow tests were conducted. From one figure it appears that 1.8×10^6 DN (60,000 RPM) was achieved with an air flow of 7.5 scfm (0.25 kg/min) and an oil flow of 5×10^{-4} gal/min (2 mℓ/min). This indicates that for an air flow increase of 12 times that the speed limit increased only from 60,000 to 72,000 RPM.

In an extensive study by SKF Industries under contract to NASA, the feasibility of using air-oil mist for emergency lubrication of 46 mm helicopter mainshaft engine bearings was investigated [12]. Oil flow rates of 20 x 10^{-4} to 22 x 10^{-4} gal/min (7.4 to 8.2 mℓ/min) and air flows of 15.5 to 20.7 scfm (0.514 to 0.686 kg/min) were used for most of the tests. The bearing was operated to 2.5 x 10^6 DN (55,000 RPM) with no apparent problem, but cage instability (cage vibration) and excessive cage wear resulted between 2.5 x 10^6 DN and 3.0 x 10^6 DN (65,000 RPM). Here it should be recalled that higher DN values are generally achievable on larger bore bearings because centrifugal effects are less severe.

An analytical approach was used in the SKF study to estimate the air and oil flow requirements; it is interesting to compare these results with the experimental results. An SKF computer program was used to calculate the bearing heat generation rate at various speeds with a 400 pound (1779 N) thrust load. Based on the theoretical heat generation rate, a 200°F (366 K) inlet air temperature, and a 500°F (535 K) bearing operating temperature, a heat transfer analysis by SKF indicated a cooling air flow requirement of 72 scfm (2.39 kg/min) at 3.0 x 10^6 DN (65,000 RPM). The bearing in fact operated with air flows of 15.5 to 20.7 scfm (0.514 to 0.686 kg/min) with outer ring temperatures of 396 to 446°F (475 to 503 K). Figure 2 from reference [12] shows the theoretical and experimental bearing heat generation rate.

The oil flow requirements were calculated by SKF based on elastohydrodynamic (EHD) lubrication theory. EHD lubrication results in cases where elastic deformation of bearing surfaces and resulting extremely

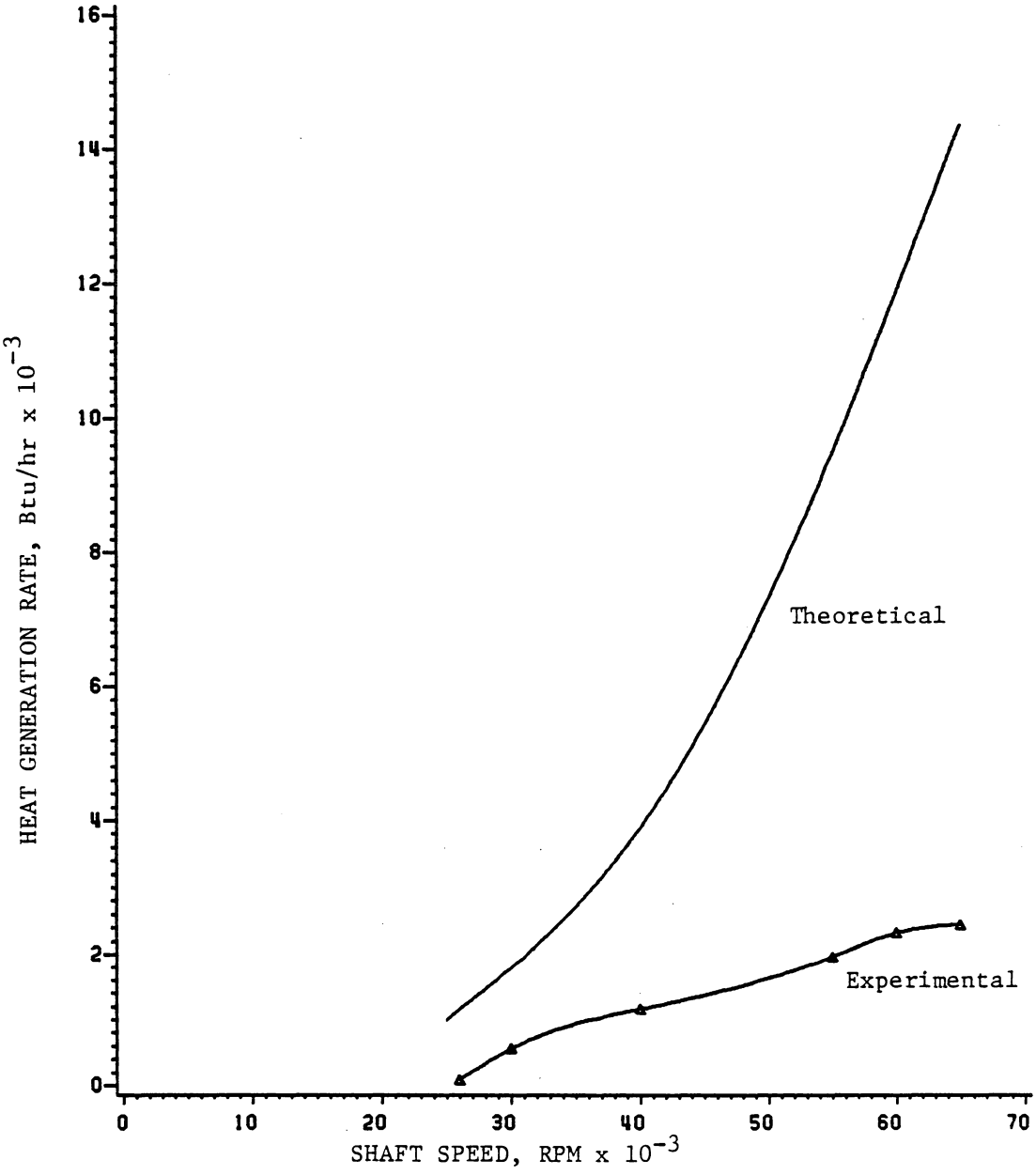

Figure 2. Theoretical and Experimental Heat Generation Rates from the SKF Study [12].

high lubricant pressures become significant, as in rolling element bearings [7]. Calculated oil flows range from 9.4×10^{-4} gal/min (3.6 mℓ/min) at 1.75×10^{6} DN to 2.4×10^{-3} gal/min (9.2 mℓ/min) at 3.0×10^{6} DN. In one group of controlled variable tests, bearing operation to 3×10^{6} DN was achieved with only 2.3×10^{-4} gal/min (0.85 mℓ/min). SKF researchers concluded that "the same quality of lubrication was obtained with the much reduced oil flow rate and that adequate lubrication was provided . . ." [11].

The differences between the analytically- and experimentally-determined cooling and lubrication requirements illustrates the need for actual bearing testing. It should also be noted that even the relatively low oil flow rate of 2.3×10^{-4} gal/min (0.85 mℓ/min) represents a sizable cost and housekeeping problem by industrial standards. For air-oil mist to be practical in many applications, both the air and oil flow must be minimized while still allowing safe bearing operation.

III. BEARING TEST RIG AND EXPERIMENTAL PROCEDURE

3.1 Test Rig Hardware

A bearing test rig was developed to drive 25 and 30 mm deep groove and angular contact ball bearings to speeds in excess of 70,000 RPM. The test rig consists of an air turbine drive coupled to a bearing test unit as shown in Fig. 3. Both the turbine and test unit are mounted on a ground steel bedplate which is mounted on a steel support table.

The turbine drive unit is an extensively modified Airesearch turbocharger turbine. The turbine is capable of developing 36 hp (27 kw) at 100,000 RPM. Modifications to the original turbocharger included removal of the compressor unit and fabrication of a new shaft and bearing housing. The new shaft and housing allowed a change from the original journal bearings to 15 mm angular contact ball bearings. This allowed a larger, stiffer shaft to be used, eliminated journal bearing stability problems, and eliminated the required oil flood lubrication system. The turbine was operated uncoupled to 75,000 RPM with no problems and minimal vibration.

The bearing test unit is an overhung housing design with the shaft mounted on two 17 mm deep groove support ball bearings. Two separate shafts and overhung housings allowed use of the same basic rig for testing both 25 and 30 mm ball bearings. The overhung housing also allowed changing both thrust and radial loads easily. Radial loading was achieved by suspending weights from a rod which was attached to the overhung housing and which passed through a hole in the bedplate. This arrangement also provided a large inertia to the overhung housing, and

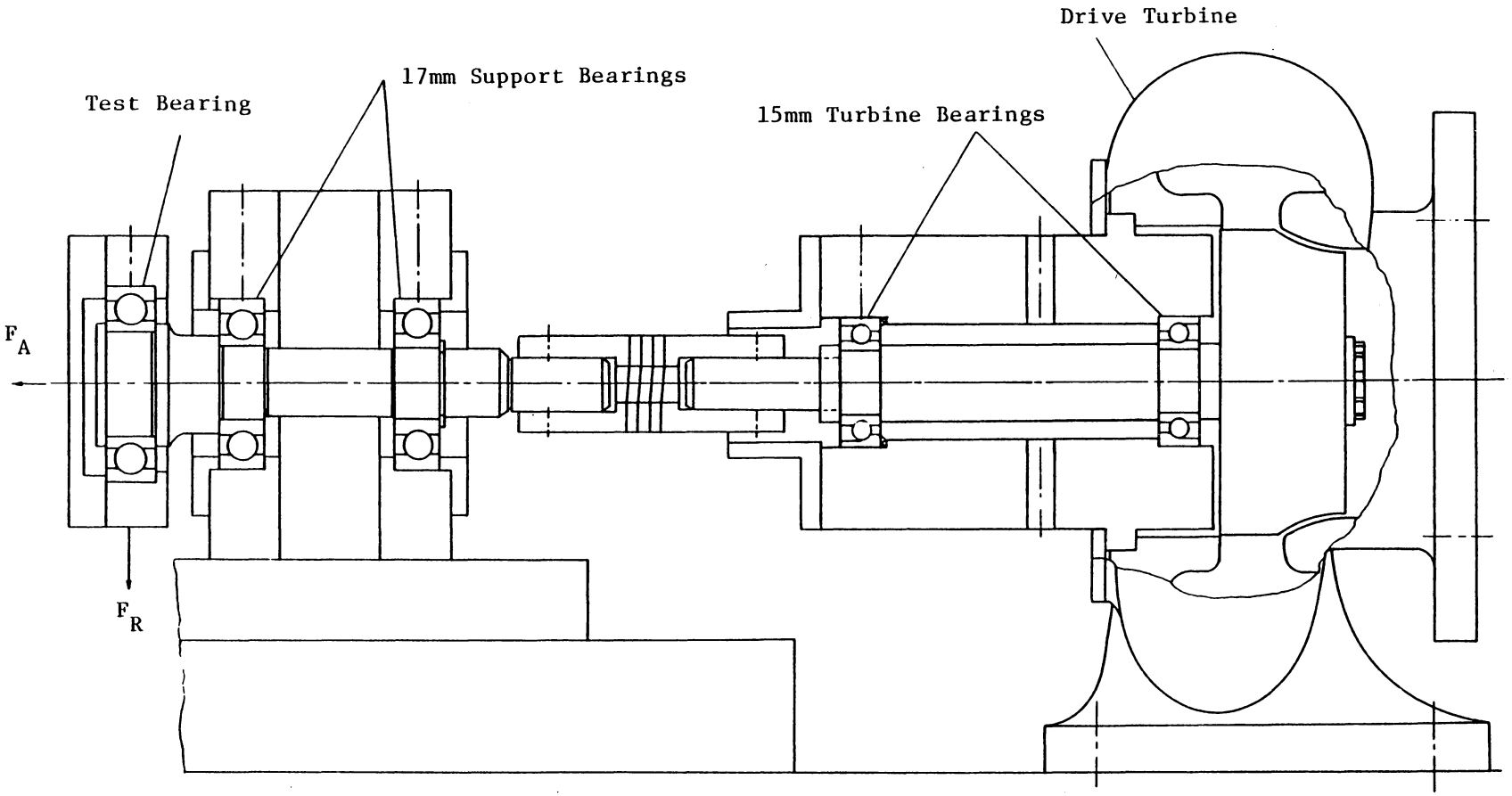

Fig. 3. High Speed Bearing Test Rig

prevented excessive rotation of the housing should a bearing seizure occur. Thrust loading was achieved by suspending weights from a cable which passed through a pulley arrangement located at one end of the support table. A strain-gaged cantilevered beam opposed rotation of the overhung housing and was intended to allow measurement of test bearing torque. Unfortunately, the torque measuring system could not be made operational for reasons to be outlined later.

While the overhung housing arrangement has been used by other investigators [5,8], vibration problems at speeds below 40,000 RPM were encountered in the present investigation (Campbell diagrams for test unit resonances are shown in Figs. A-2 to A-4 of Appendix A). Very low support bearing damping, and close spacing of the support bearings relative to the overhung shaft length are believed to be causes for the vibration problems.

The test unit was coupled to the air turbine drive by a flexible coupling manufactured by the Helical Products Company. Three of these couplings were donated to this project by Helical Products. The coupling was made from a single cylindrical piece of 17-4 PH stainless steel with a spiral helix cut in the midsection to provide the flexible element. The coupling was balanced by the Industrial Drives Division of Kollmorgen Corporation to allow high speed operation. With a 0.875 inch (22.2 mm) outside diameter and a 0.50 inch (12.7 mm) bore, operation to speeds of 70,000 to 90,000 RPM should be no problem from a centrifugal stress standpoint, as can be shown by calculation. Any misalignment, however, will cause cyclical stresses in the flexible helical section of the coupling that could lead to a fatigue failure. A coupling fatigue

failure was experienced prior to the final turbine design; poor alignment and high turbine vibrations were assumed to be the cause of this failure. With the final turbine design, very good alignment and low turbine vibration were achieved, and no coupling problems were encountered during the more than 30 hours of operation during test runs.

To provide cooling and lubrication to the various rig bearings, three separate air-oil mist generators and air pressure regulators with built-in 5 micron air filters were used. One air-oil mist generator was dedicated to the drive turbine, one to the test unit support bearings, and one to the 25 or 30 mm test bearing. The air-oil mist generators allowed separate adjustment of both the air flow and oil drip rate to optimize the cooling and lubrication to the bearing.

3.2 Test Rig Instrumentation

Test rig instrumentation included speed indication, turbine vibration indication, various temperature measurements, and cooling air flow rate measurement. A Bently-Nevada proximeter transducer and a frequency counter were used for speed indication. The transducer picked up a three-per-revolution pulsation caused by three set screws on the bearing test unit end of the coupling. The frequency counter then displayed the frequency of the pulsations in kHz. A convenient scale factor of 20,000 times the displayed frequency in kHz gave the speed in RPM.

Drive turbine shaft vibration was monitored with another proximeter transducer mounted in the turbine bearing housing at approximately the midspan location between the two turbine bearings. This transducer provided a 420 mV/10^{-3} inch (420 mV/25.4 μm) signal that was read with a digital voltmeter.

One of the 15 mm turbine bearings, both 17 mm test rig unit support bearings, and the 25 or 30 mm test bearing each had a thermocouple in direct contact with the bearing outer race. One thermocouple was also in contact with the outside surface of the overhung test bearing housing. This was used to verify that the housing was in approximate thermal equilibrium with the test bearing outer race. All thermocouples were Type K (Chromel-Alumel) with direct, compensated readout provided by a multichannel Omega digital thermometer.

Cooling air flow measurement was provided by Brooks Rotameter-type flowmeters mounted downstream of the pressure regulators and just upstream of the air-oil mist generators. One rotameter was used for the 25 or 30 mm test bearing and one for both 17 mm support bearings. These flowmeters had 10 to 100 linear scales with scale factors for various operating pressures shown in Table 1.

Attempts were made to measure test bearing torque with a strain gage bridge mounted on the test housing anti-rotation beam mentioned previously. Unlike oil-jet-lubrication bearings, torque levels in air-oil mist lubricated bearings are relatively low. With the measurement equipment used in this investigation, the high rig vibrations, and friction torque introduced by the application of the test bearing loads, these low torque levels resulted in unrepeatable torque readings.

3.3 Test Bearings

All test and support bearings used in this investigation were class ABEC 7 precision ball bearings manufactured by the Barden Corporation. The test bearings were 100 "light" series ball bearings and included a

Table 1. Flowmeter Scale Factors for Various Pressures

Pressure, lb/in^2 (Gage)	Scale Factor
0	.0756
1	.0781291
2	.0805789
3	.0829564
4	.0852676
5	.0875178
6	.0897115
7	.0918529
8	.0939455
9	.0959925
10	.0979967
15	.1074586
20	.1161523
25	.1242391
30	.1318308
35	.1390085
40	.1458333
45	.1523527
50	.1586044
60	.1704211
70	.1814700
80	.1918837
90	.2017607
100	.2111761
125	.2330566
150	.2530521
175	.2715794
200	.2889210

25 mm deep groove, a 25 mm angular contact, a 30 mm deep groove, and a 30 mm angular contact bearing. Selected test bearing specifications are shown in Table 2. Test unit support bearings were 17 mm, deep groove, 200 series ball bearings. Support bearing specifications are also shown in Table 2.

All deep groove bearings had two-piece riveted construction phenolic cages. The angular contact bearings had one-piece phenolic cages. All bearing cages were of the outer-race-guided type.

3.4 Test Conditions

Test conditions for each of the four test bearings included three load configurations and three air-oil mist flow rates for a total of 36 test runs. A constant radial load of 25 pounds (111 N) was used for all tests with thrust loads of 50, 75 and 100 pounds (222, 334 and 445 N). Because of the configuration of the test shaft, the constant radial load and the three thrust loads imposed on the test bearing resulted in different radial and thrust loads to the 17 mm support bearings. The support bearing nearest the overhung housing had constant radial and thrust loads of 38 and 21 pounds (169 and 93 N), respectively. The coupling end support bearing had a constant radial load of 13 pounds (58 N), and thrust loads of 71, 96, and 121 pounds (316, 427, and 538 N) for test bearing thrust loads of 50, 75, and 100 pounds (222, 334, and 445 N), respectively.

Air flow rates to the test bearing air-oil mist generator of 1.5, 3.0, and 6.0 scfm (0.05, 0.10, and 0.20 kg/min) were used. A single air flow rate of 1.5 scfm (0.05 kg/min) was used for both 17 mm support

Table 2. Test and Support Bearing Specifications

	Deep Groove Bearings			Angular Contact Bearings	
Bore, mm	17 mm	25 mm	30 mm	25 mm	30 mm
Outside Diameter, mm	40	47	55	47	55
Pitch Diameter, in.	1.1222	1.4165	1.6900	1.4165	1.6900
Catalog Speed, RPM	58,800	42,500	35,400	42,500	35,400
Contact Angle, °	14.8	15.2	12.2	14.5	15.3
Radial Clearance, in.	0.0005 to 0.0009	0.0005 to 0.0009	0.0005 to 0.0009	0.0007 to 0.0011	0.0007 to 0.0011
Inner Race Curvature	0.52	0.52	0.515	0.52	0.515
Outer Race Curvature	0.52	0.52	0.54	0.53	0.53
Ball Complement	8	10	11	13	14
Ball Size, in.	17/64	1/4	9/32	1/4	9/32

bearings for most of the tests. After the air passed through the support bearing air-oil mist generator, the air-oil mist flow was divided through a wye connection to provide 0.75 scfm (0.025 kg/min) of air to each support bearing.

The oil flow rate was set at 60 drops/min through the sight dome of the mist generators for all tests, but the actual oil flow rate to the bearings varied with each air flow. Oil flow rates of 1.4×10^{-5}, 1.24×10^{-5} and 3.14×10^{-5} gal/min (0.051, 0.047 and 0.119 ml/min) for air flows of 1.5,, 3.0, and 6.0 scfm (0.05, 0.10, and 0.20 kg/min), respectively, were measured for the test bearing air-oil mist generator. The oil flow to each of the 17mm support bearings was assumed to be 0.7×10^{-5} gal/min (0.026 ml/min), one half of the oil flow associated with the 1.5 scfm (0.05 kg/min) air flow above.

A petroleum-based lubricant, "Mobil DTE Light", was used for all tests. Table 3 shows selected specifications of this oil.

A 0.129 inch (3.28 mm) diameter reclassifying nozzle was used for the test bearing, and a 0.093 inch (2.36 mm) nozzle was used for each 17 mm support bearing. The test bearing reclassifying nozzle was threaded on the outside diameter. This permitted the nozzle to be rigidly attached to the end cover plate of the overhung housing. The air-oil mist discharged from the nozzle into a space between the cover plate and the test bearing. This forced the air-oil mist to pass through the test bearing in order to achieve maximum cooling and lubrication. The support bearing reclassifying nozzles were directed at the gap between the bearing cage and inner race and were located approximately 0.25 inch (6.4 mm) from the bearing. Air-oil mist was not forced through the

Table 3. Specifications of Lubricant Used During Testing

Manufacturer	Mobil
Lubricant Trade Name	DTE Light
150/VG Grade	32
ASTM Viscosity Grade	150
Viscosity, CST @ 40°C	30.4
Viscosity, CST @ 100°C	5.3
Pour Point, °F	20
Viscosity Index	100
ASTM Color	1.5

support bearings.

The pressure just upstream of the test bearing reclassifying nozzle was measured during several test runs. Pressures of 4.5, 11.5, and 31.0 psig (31, 75.8, and 214 kPa) were measured for air flows of 1.5, 3.0, and 6.0 scfm (0.05, 0.10, and 0.20 kg/min), respectively. Based on these pressures and approximately atmospheric discharge pressure, the nozzle would be in a choked condition at the 6.0 scfm (0.20 kg/min) air flow rate.

3.5 Test Procedure

Test runs were conducted by first establishing the air-oil mist flow to the test and support bearings, and then setting the bearing thrust load. The rig was then brought up to some nominal speed, usually about 20,000 RPM, and allowed to operate until all temperatures stabilized, about 15 to 20 minutes. Temperatures were recorded, the speed increased, and again temperatures were allowed to stabilize. Most test runs were terminated when the test bearing outer race temperature reached approximately 200°F (366 K), although some tests were run to 240°F (389 K).

The limiting temperature was established based on both experience and lubricant viscosity at operating temperature. During the development of the test rig, several preliminary runs were conducted in which the test bearing temperature exceeded 250°F (394 K). Visual inspection of the bearing and housing revealed brownish deposits indicating lubricant degradation. Further, adequate lubricant viscosity is required at operating temperature to provide the EHD lubricant film to prevent

metal to metal contact between the balls and races. The Barden Bearing Catalog (13) gives a simple equation that can be used to estimate the required lubricant viscosity for a given set of bearing parameters. The lubricant used during testing typically just satisfied the viscosity requirements at 212°F (373 K).

Frequently high vibrations were encountered during testing, especially below about 40,000 RPM, which made rig operation difficult. Speeds at which these high vibrations occurred were inconsistent, and not always associated with the calculated rig critical speeds. Because of these high vibrations, the rig could not always be operated at convenient speed increments, thus complicating the testing and later the data analysis.

The general testing procedure outlined above was repeated for each load and flow condition for a total of nine test runs on each bearing. Between each test, the overhung housing was disassembled, the test bearing visually inspected, and the next bearing installed. When changing from the 25 to the 30 mm test bearings, the test rig shaft and housing were also changed.

IV. RESULTS

Test results for the four test bearings under various load and air-oil mist flow conditions are presented graphically in this chapter. Support bearing results are also presented for three load conditions, although the air-oil mist flow remained constant for all the test runs.

All figures show stabilized bearing outer race temperature versus shaft rotational speed. Figures 4, 5 and 6 show results for the 25 mm deep groove bearing at 1.5, 3.0 and 6.0 scfm (0.05, 0.10, and 0.20 kg/min) air flows, respectively, under varying loads. Figures 7, 8, and 9 again show results for the 25 mm deep groove, but at 50, 75 and 100 pound (222, 334, and 445 N) thrust loads, respectively, and varying air-oil mist flows. A similar format is used in Figs. 10 through 15 for the 25 mm angular contact bearing, Figs. 16 through 21 for the 30 mm deep groove bearing and Figs. 22 through 27 for the 30 mm angular contact bearing. Before discussing specific results, a brief discussion of generally expected results should be made.

Typically an increase in bearing temperature is expected as speed is increased, load is increased, or air-oil mist flow is decreased. As speed is increased there is a point at which the temperature might sharply increase due to reduced bearing clearances, loss of EHD lubricant film, ball skidding against the races, cage instability or vibration, or a combination of these effects. It is uncertain if stabilized temperatures could be maintained at significantly higher speeds. In general, the test data supported these expectations, but there were inconsistencies.

Figures 4 through 6 for the 25 mm deep groove bearing show that for all three flow conditions higher temperatures resulted from higher loads. Temperature differences due to load were more pronounced at the 1.5 scfm (0.05 kg/min) air flow than at the 3.0 and 6.0 scfm (0.10 and 0.20 kg/min) air flows. For a given load, Figs. 7, 8, and 9 show significantly higher temperatures for the low air flow condition while temperature differences between the 3.0 and 6.0 scfm (0.10 and 0.20 kg/min) flows were much less pronounced. Figure 6 most clearly shows a sharp rise in temperature at high speeds.

Results from the 25 mm angular contact bearing were not as consistent as results from the deep groove bearing. For a given air flow, there was little temperature variation with load (see Figs. 10, 11, and 12). However, for a given load, the low air flow condition resulted in a much higher temperature than the two higher air flows (see Figs. 13, 14, and 15). At 40,000 RPM and a 75 pound thrust load, for example, the outer race temperature was 211°F (372 K) for 1.5 scfm (0.05 kg/min) and about 135°F (330 K) for 3.0 and 6.0 Scfm (0.10 and 0.20 kg/min), as shown in Fig. 14.

For the 30 mm deep groove bearing, operation was not possible above 25,000 RPM with a 1.5 scfm (0.05 kg/min) air flow without exceeding 200°F (366 K), as is apparent in Fig. 16. This is 10,000 RPM below the catalog limiting speed. Excessive test rig vibration at lower speeds is believed to have contributed to this poor performance. This is supported by Fig. 17 where the temperature actually dropped as the speed increased from 24,000 to 31,000 RPM for the 3.0 scfm, (0.10 kg/min) air flow and 75 pound (334 N) load, while the temperature remained almost

constant for 50 and 100 pound (222 and 445 N) load conditions. Much better performance was achieved for the 3.0 and 6.0 scfm (0.10 and 0.20 kg/min) air flows as shown in Figs. 11 and 12. In these particular test runs, a brief rig performance test was conducted in which the bearing outer race temperature was allowed to exceed 200°F (366 K). A stable operating temperature of 240°F (389 K) was achieved at 60,000 and 63,200 RPM for 6.0 and 3.0 scfm air flow rates, respectively. This is about 1.8 times the catalog speed rating. The rig was then operated at 70,080 RPM for two minutes, but the test bearing temperature rapidly rose to 251°F (395 K) and did not stabilize. Figures 19 through 21 again show the marked difference in bearing temperature for the low air flow condition.

The poorest performance in terms of temperature at any given load, air-flow, and speed was obtained with the 30 mm angular contact bearing. Similar performance to the 30 mm deep groove bearing was observed for the 1.5 scfm (0.05 kg/min) air flow condition (Fig. 22), but no significant improvement was achieved with 3.0 scfm (0.10 kg/min) as shown in Fig. 23. Increasing the air flow to 6.0 scfm (0.20 kg/min) allowed the bearing to be run above 30,000 RPM, and although the outer race temperature exceeded 210°F (372 K) the rate of temperature rise decreased for the 75 pound and 100 pound (334 and 445 N) loads (Fig. 24). This is not typically expected performance, and is believed to have been caused in part by test rig vibrations at the lower speeds. The 50 pound (222 N) load condition shows a sharp increase in temperature at 35,000 to 40,000 RPM, very different from the 75 and 100 pound (334 and 445 N) conditions. This difference may be due to ball skidding

at the lower load condition. Temperature variation with air flow is not as significant with the 30 mm angular contact bearing as with the other bearings tested as seen in Figs. 25 through 27.

A summary of the maximum speed achieved with each test bearing, both with stable and increasing outer race temperatures, is presented in Table 4. These data do not imply that greater speeds cannot be achieved, but only reflect the speeds attained before test termination due to the bearing outer race temperature exceeding some value judged to be excessive (usually about 200°F).

As mentioned previously, data were taken on the 17 mm support bearings, although the air flow remained constant at 0.75 scfm (0.025 kg/min) per bearing for all of the tests. Initially, the test program plan was to vary the air-oil mist flow to the support bearings also, but the air flow used was approximately the minimum flow that could accurately be measured on the flowmeter. Even this low air flow resulted in much lower support bearing temperatures than the 25 and 30 mm test bearings, as shown in Figs. 28 through 30. Higher air flows also caused a fine oil-mist to fill the laboratory since the support bearing oil-mist nozzles were not discharged into an enclosed housing as with the 25 and 30 mm test bearings. Incidentally, this indicates that some oil is not being used to lubricate the bearing even when using reclassifying nozzles.

Figures 28, 29 and 30 show the outer race temperatures for the support bearing nearest the drive coupling. This bearing supported the thrust load applied to the test bearing as well as the thrust from a wave spring used to preload the other support bearing. A close compari-

Table 4. Summary of Maximum Test Bearing Speeds Achieved

25mm Deep Groove		
60,400 RPM (1.51×10^6 DN)	208°F	(Stable)
64,000 RPM (1.60×10^6 DN)	230°F	(Increasing)
25mm Angular Contact		
56,000 RPM (1.40×10^6 DN)	208°F	(Stable)
30 mm Deep Groove		
63,200 RPM (1.90×10^6 DN)	240°F	(Stable)
70,080 RPM (2.10×10^6 DN)	251°F	(Increasing)
30mm Angular Contact		
42,000 RPM (1.26×10^6 DN)	203°F	(Stable)
46,000 RPM (1.38×10^6 DN)	235°F	(Increasing)

son of the curves (generated using a cubic regression curve fitting routine) show that temperature increases as load is increased, but the increase is relatively small. The data also have a much wider "spread" at lower RPM which may be the result of inconsistent rig vibrations at low speeds. In general, it is apparent that the 17 mm support bearings were not being operated to their full potential at the speeds tested.

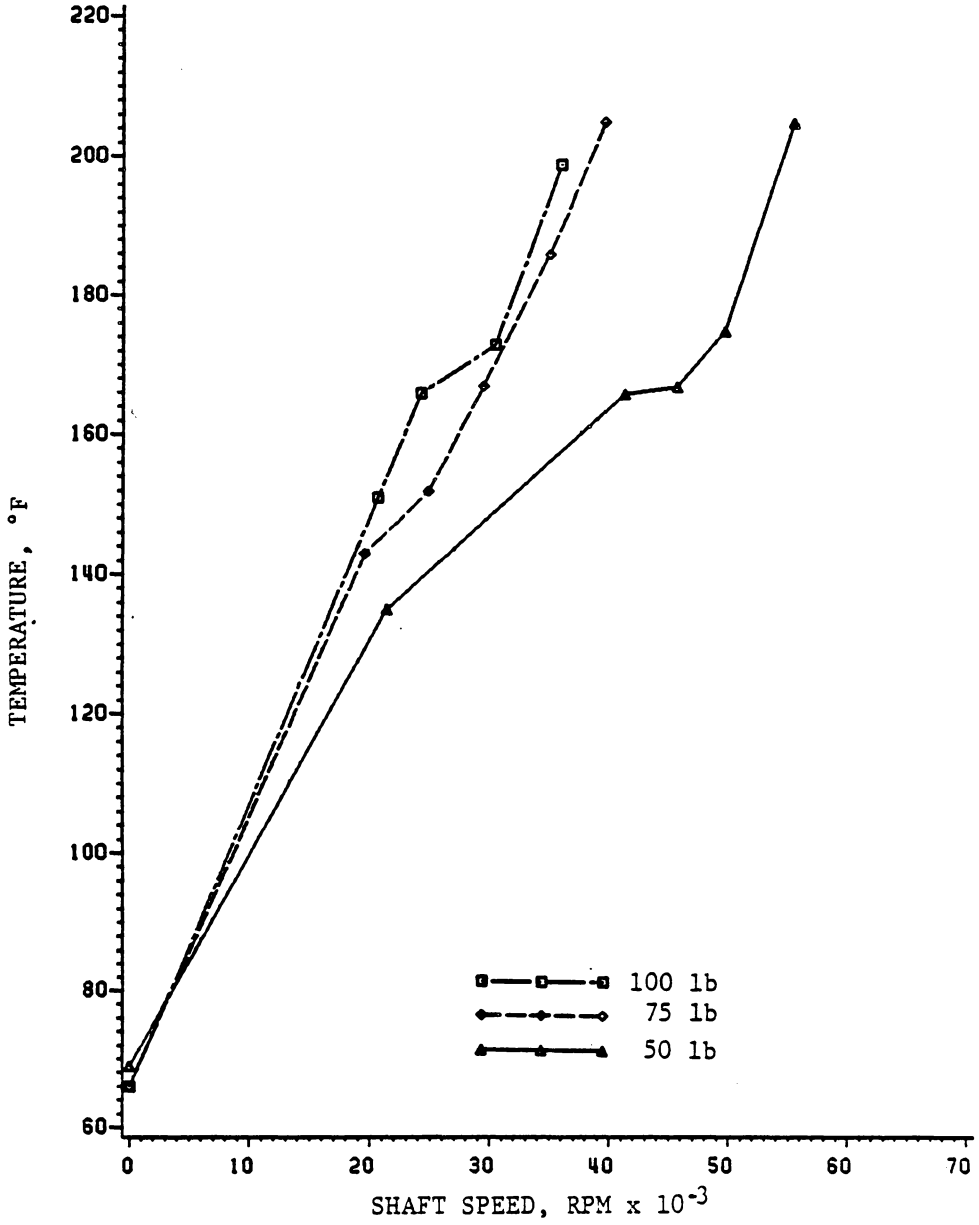

Fig. 4. Test Results for the 25mm Deep Groove Bearing with a 1.5 scfm Air Flow.

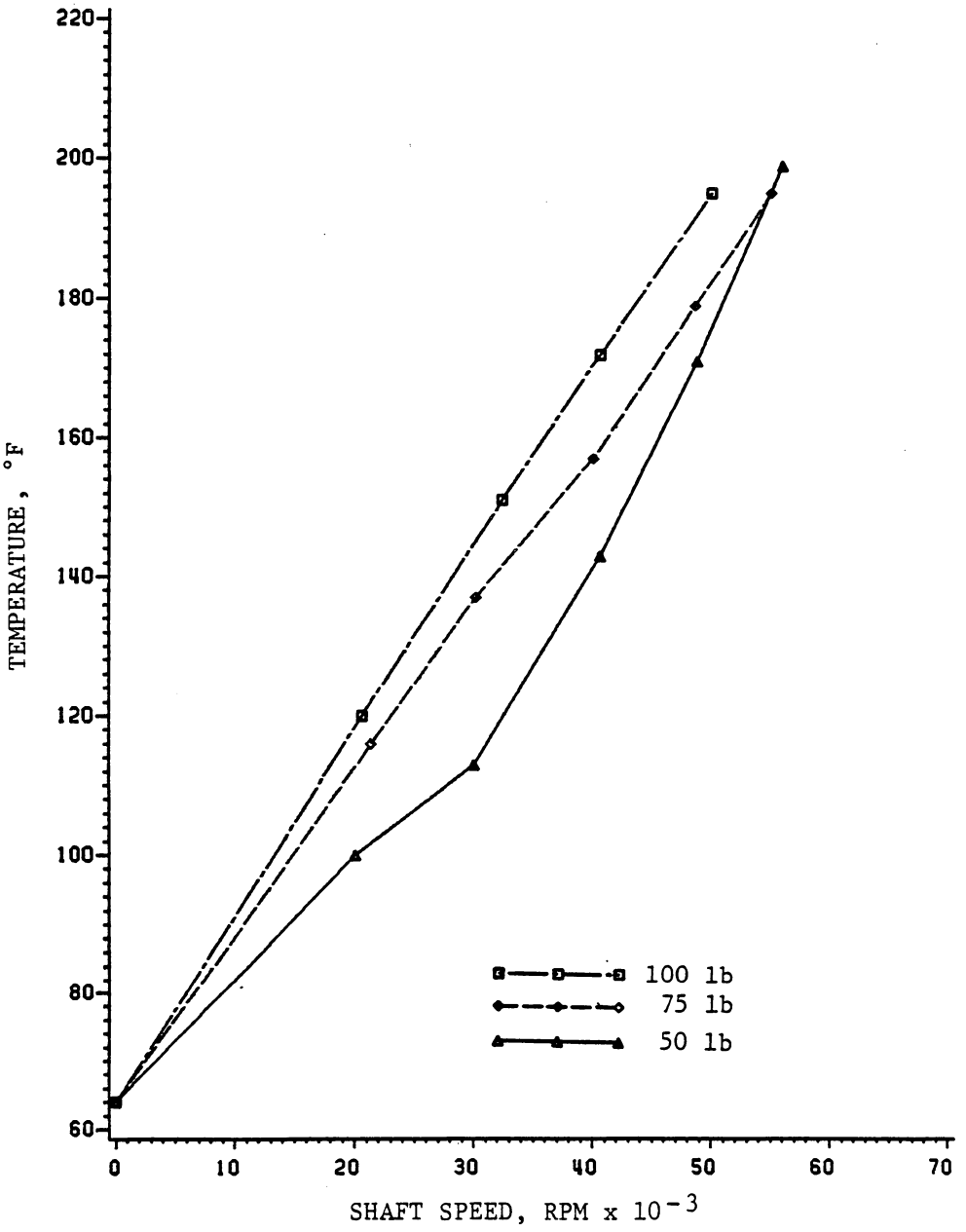

Fig. 5. Test Results for the 25mm Deep Groove Bearing with a 3.0 scfm Air Flow.

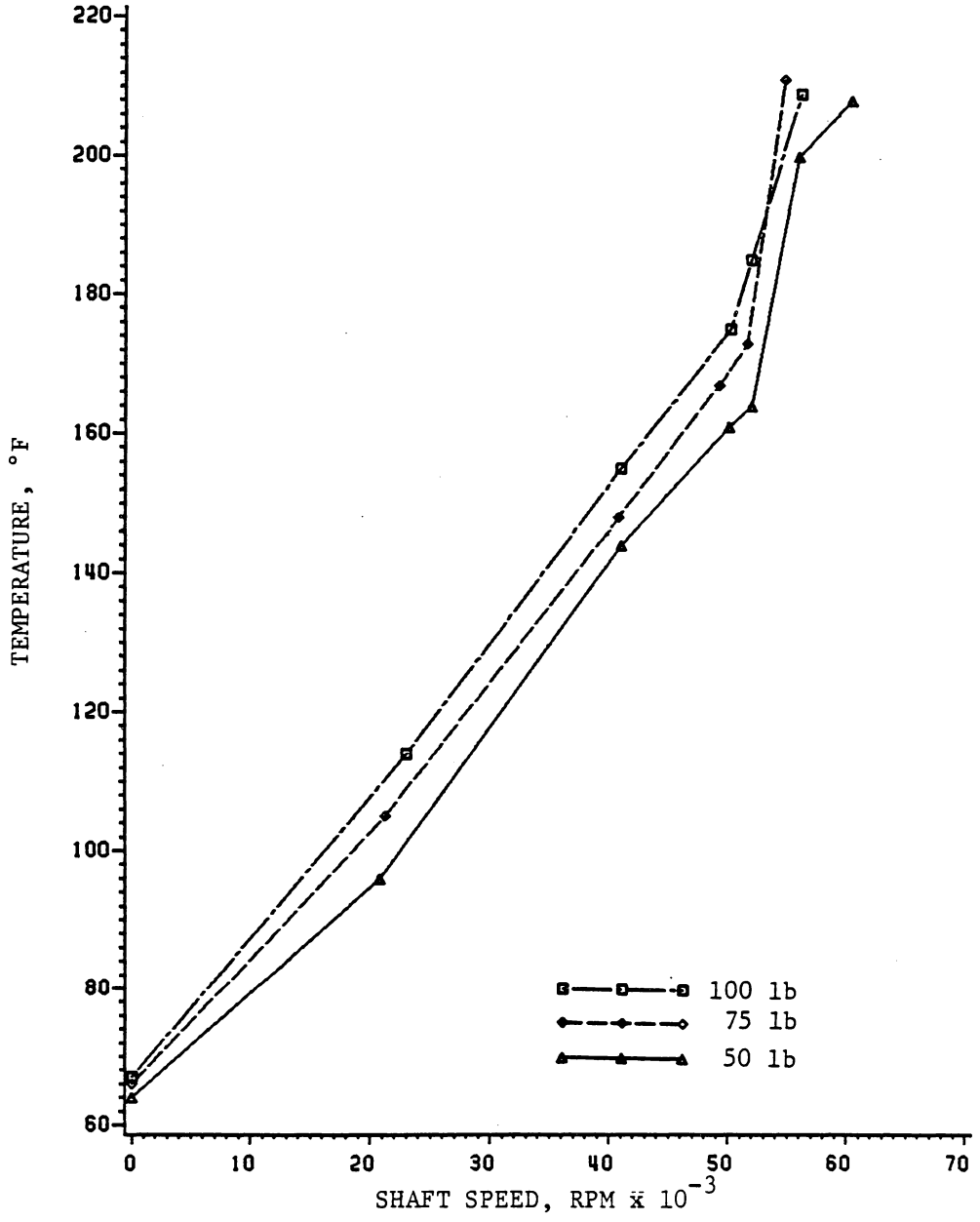

Fig. 6. Test Results for the 25mm Deep Groove Bearing with a 6.0 scfm Air Flow.

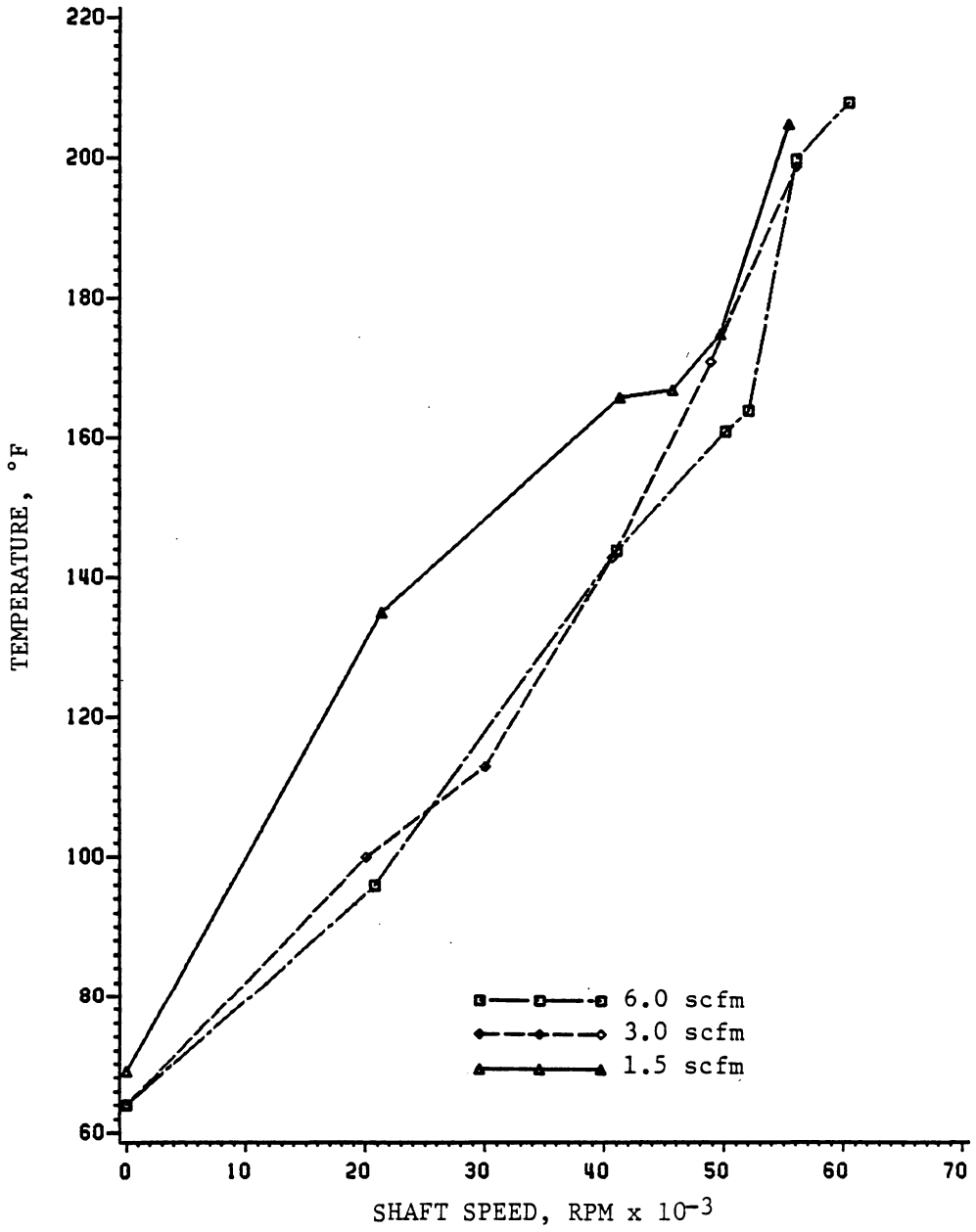

Fig. 7. Test Results for the 25mm Deep Groove Bearing with a 50 lb Thrust Load.

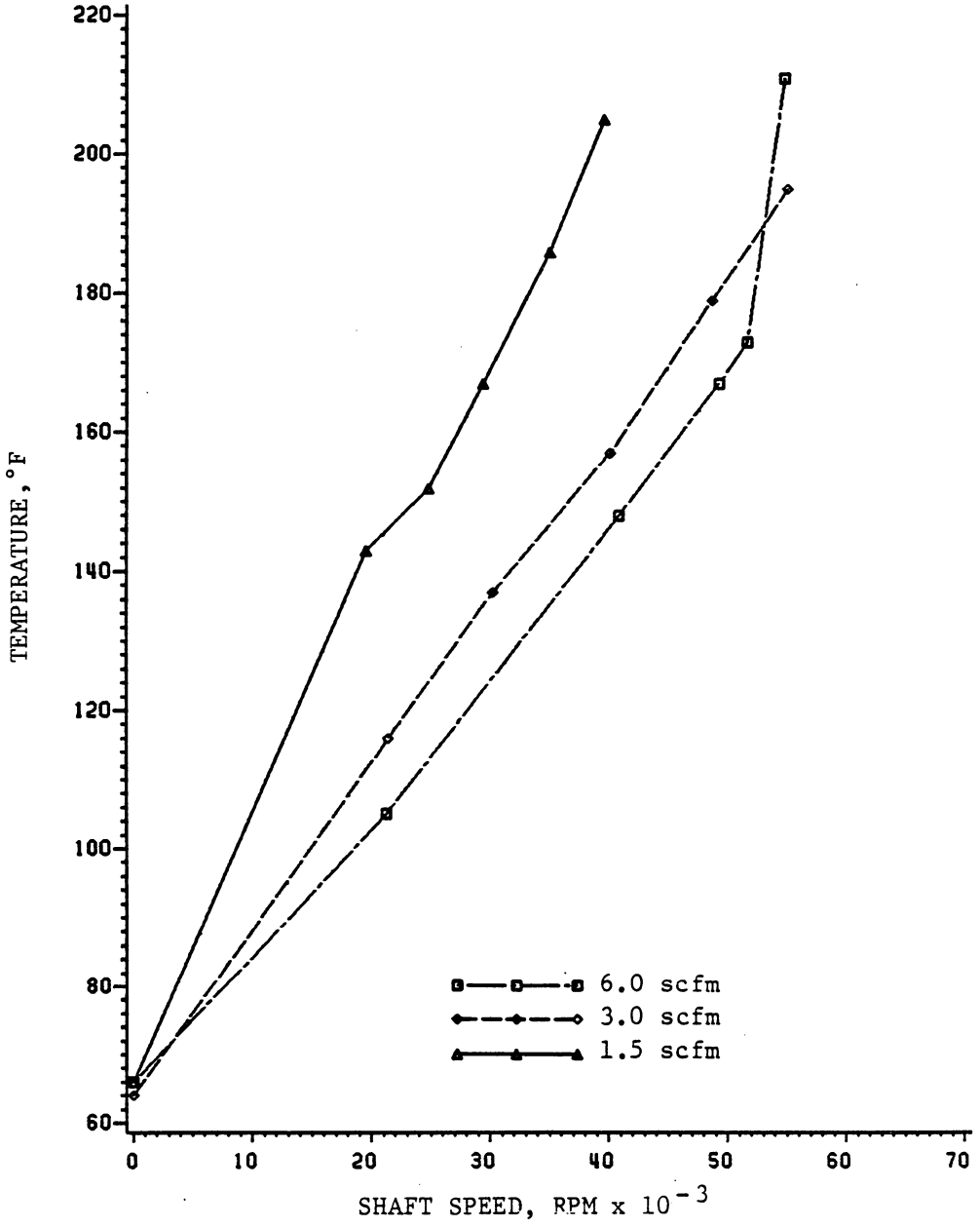

Fig. 8. Test Results for the 25mm Deep Groove Bearing with a 75 lb Thrust Load.

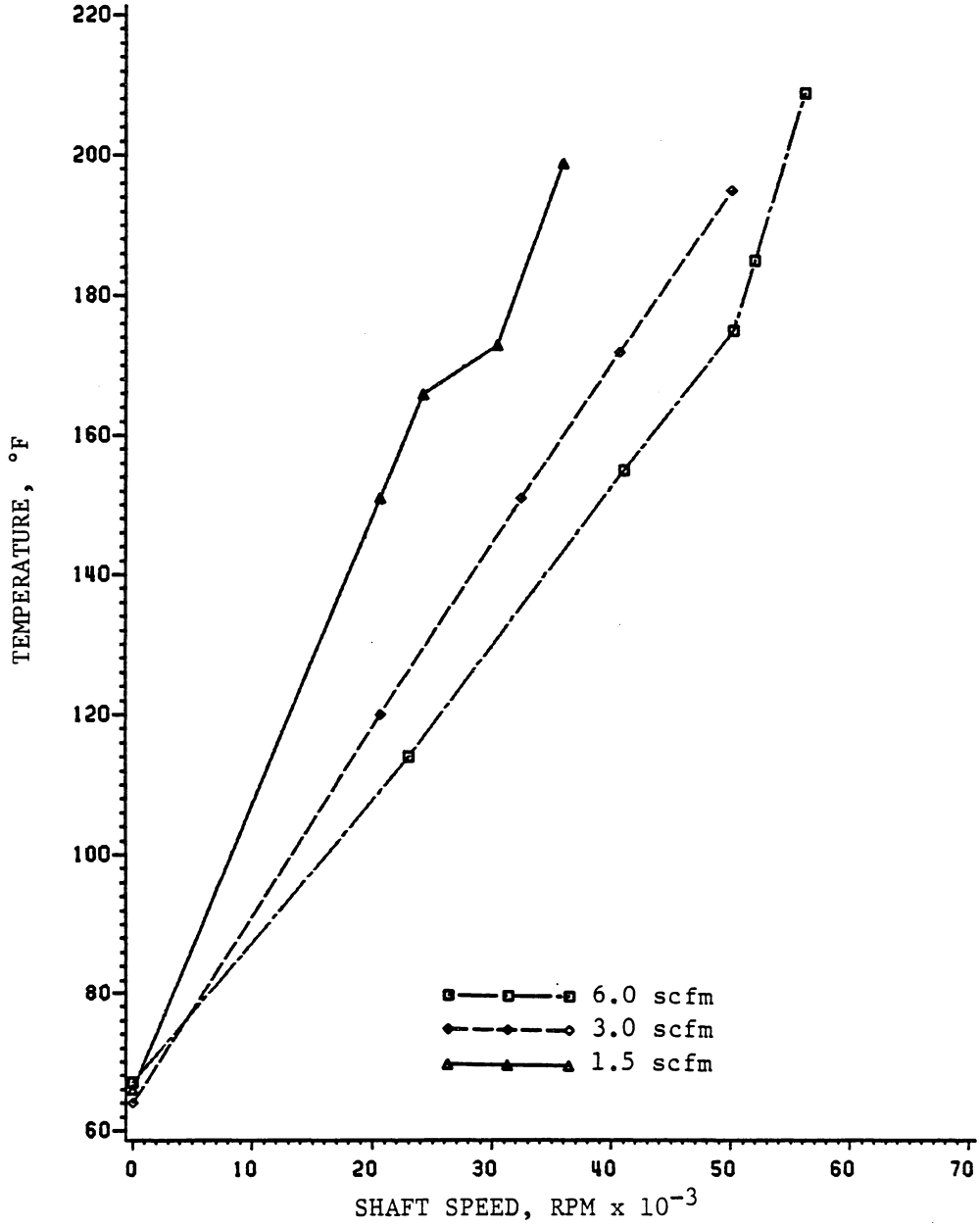

Fig. 9. Test Results for the 25mm Deep Groove Bearing with a 100 lb Thrust Load.

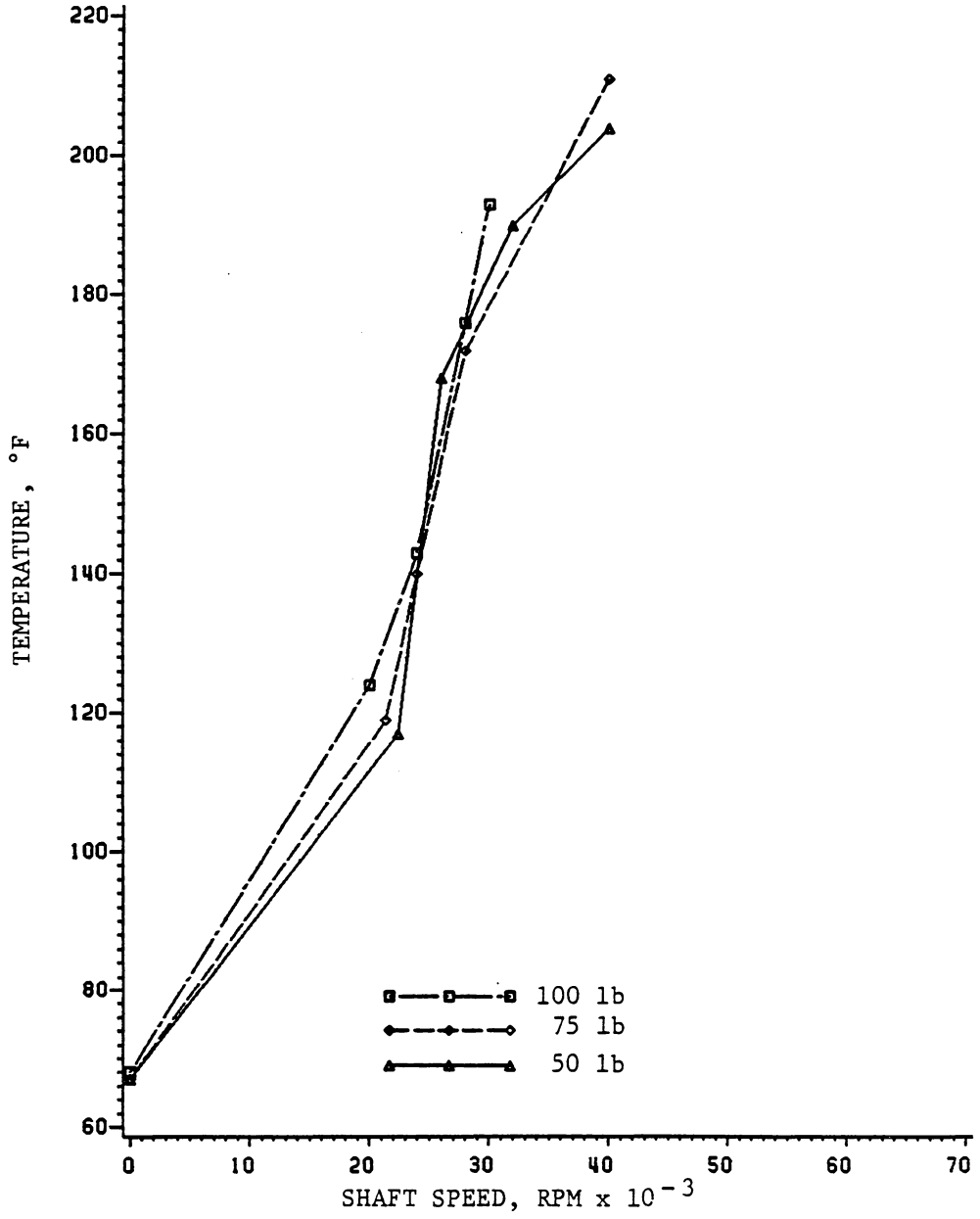

Fig. 10. Test Results for the 25mm Angular Contact Bearing with a 1.5 scfm Air Flow.

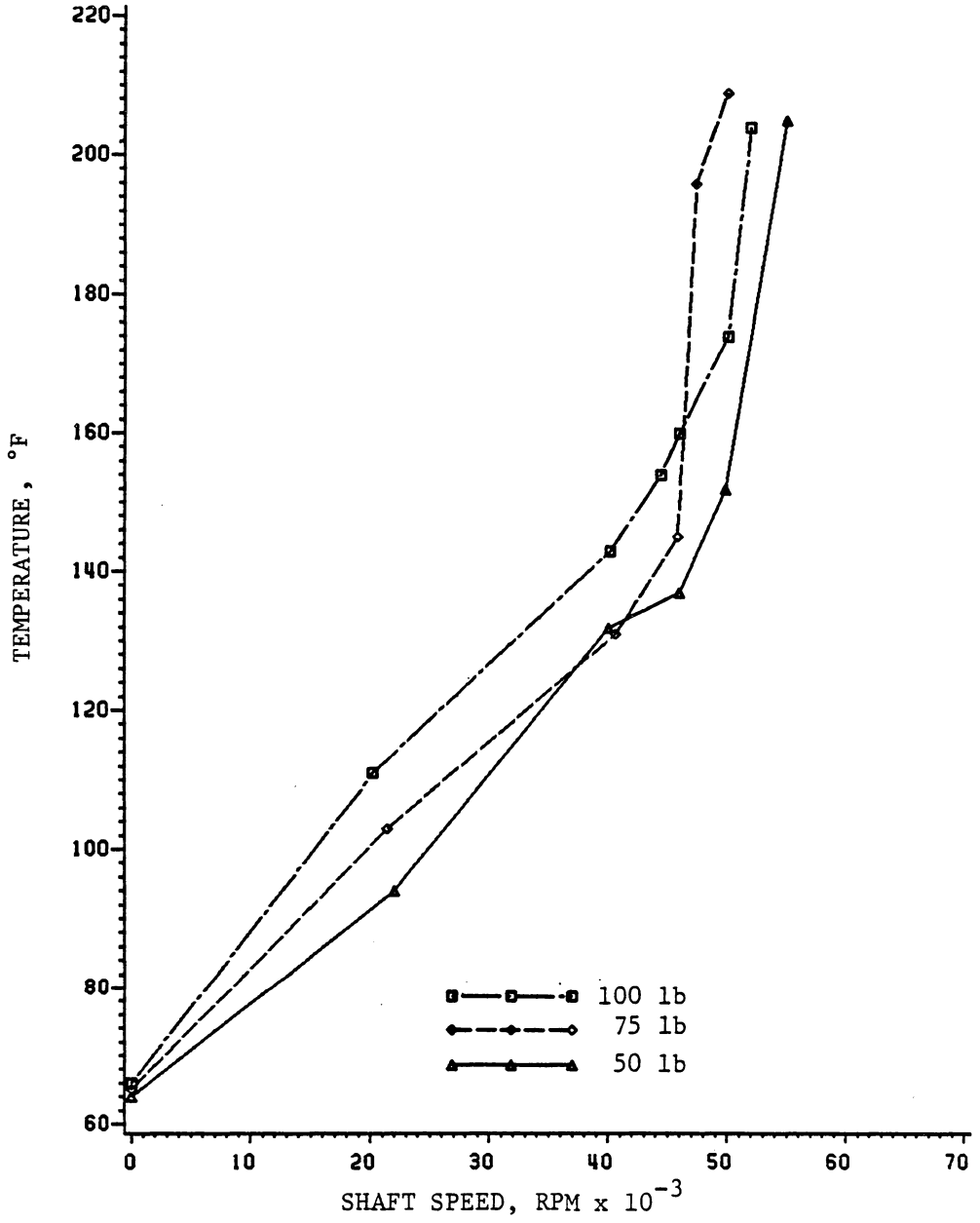

Fig. 11. Test Results for the 25mm Angular Contact Bearing with a 3.0 scfm Air Flow.

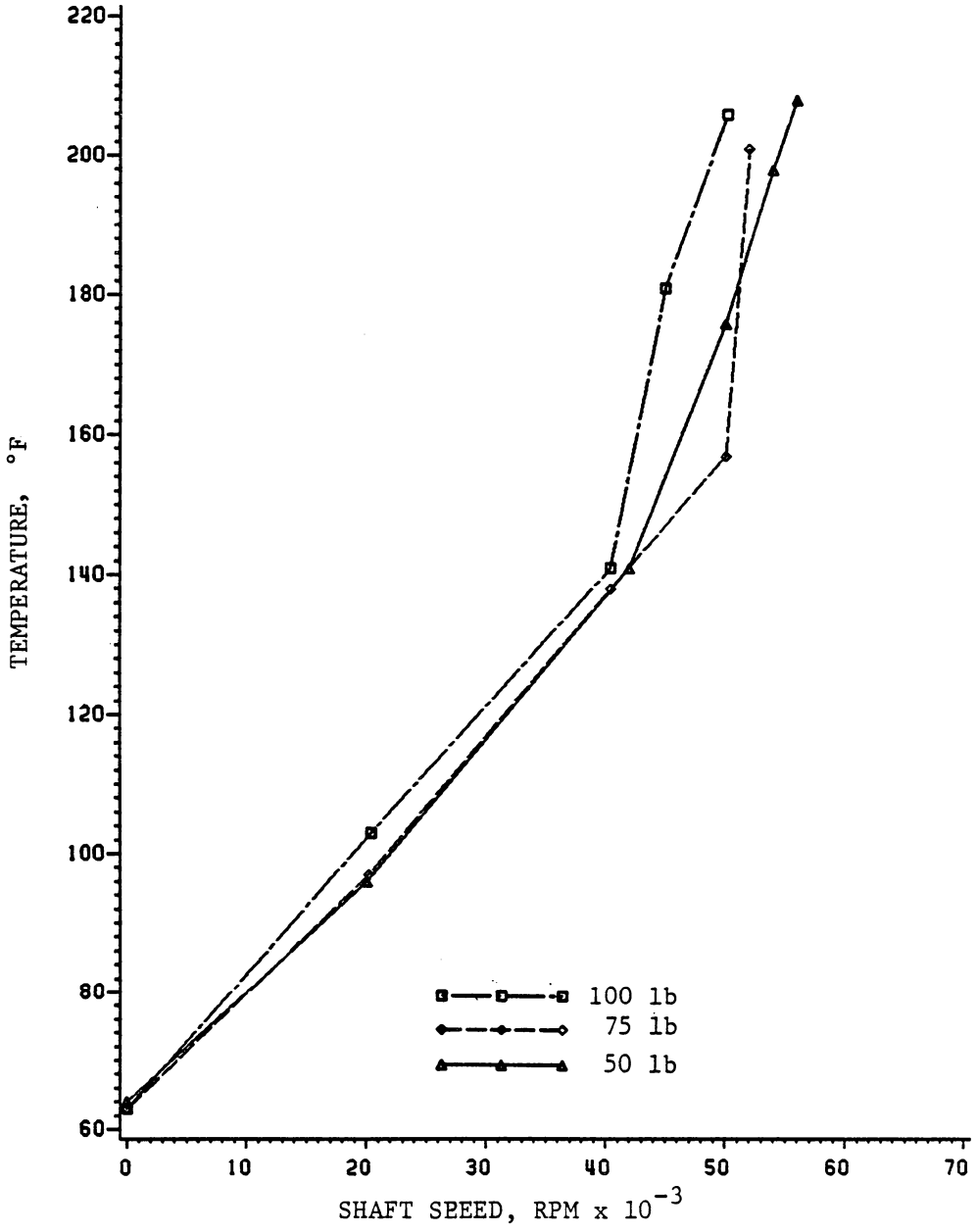

Fig. 12. Test Results for the 25mm Angular Contact Bearing with a 6.0 scfm Air Flow.

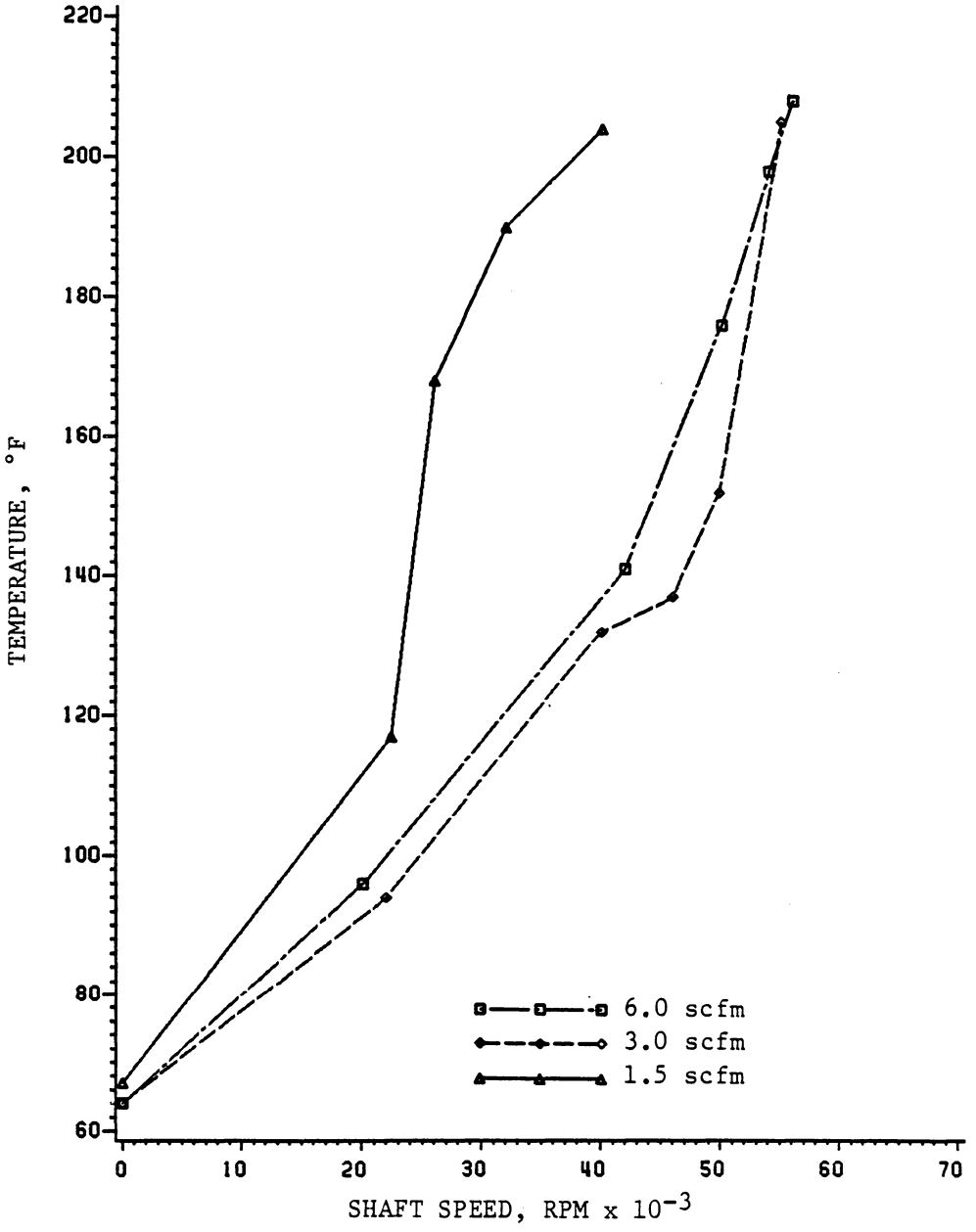

Fig. 13. Test Results for the 25mm Angular Contact Bearing with a 50 lb Thrust Load.

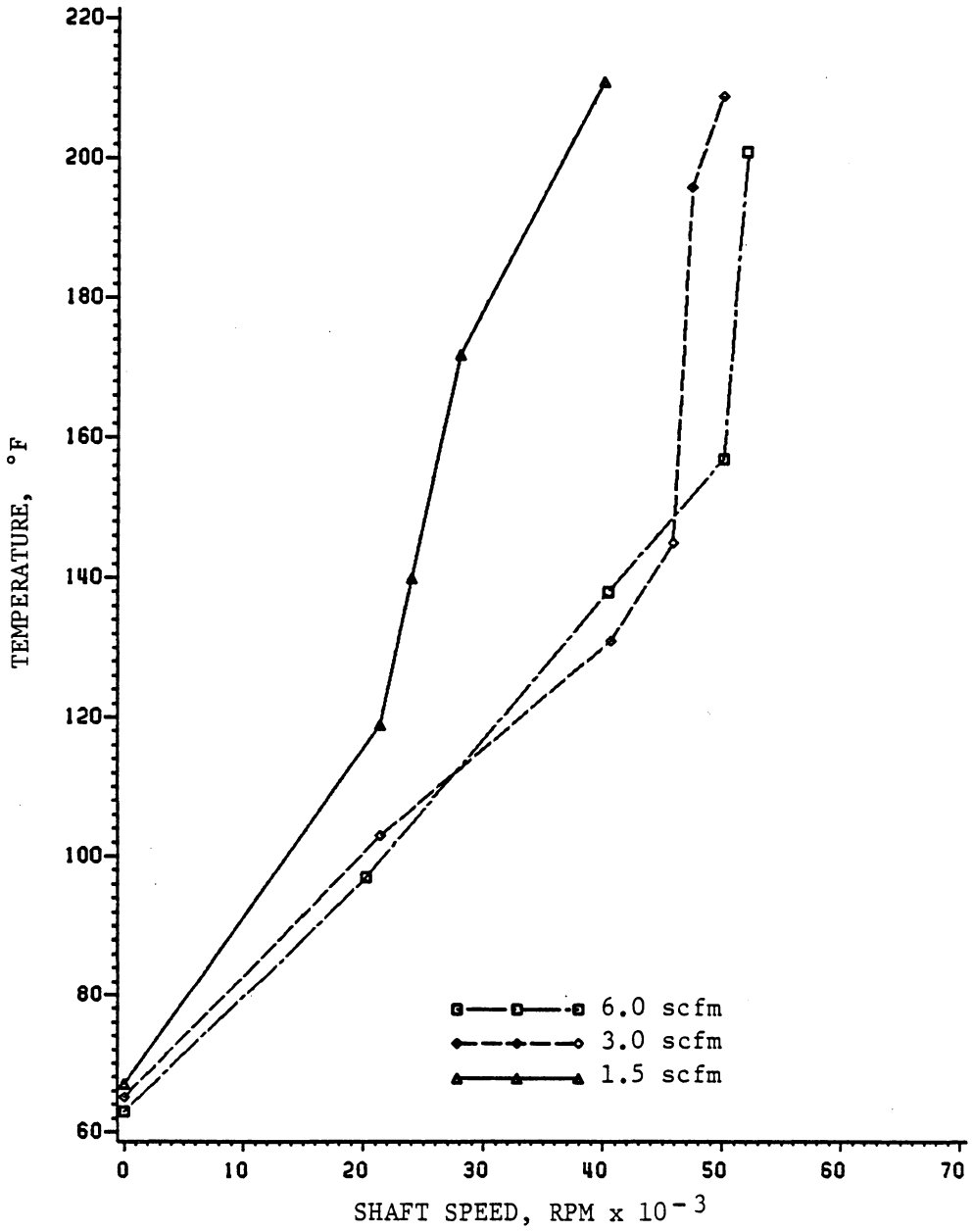

Fig. 14. Test Results for the 25mm Angular Contact Bearing with a 75 lb Thrust Load.

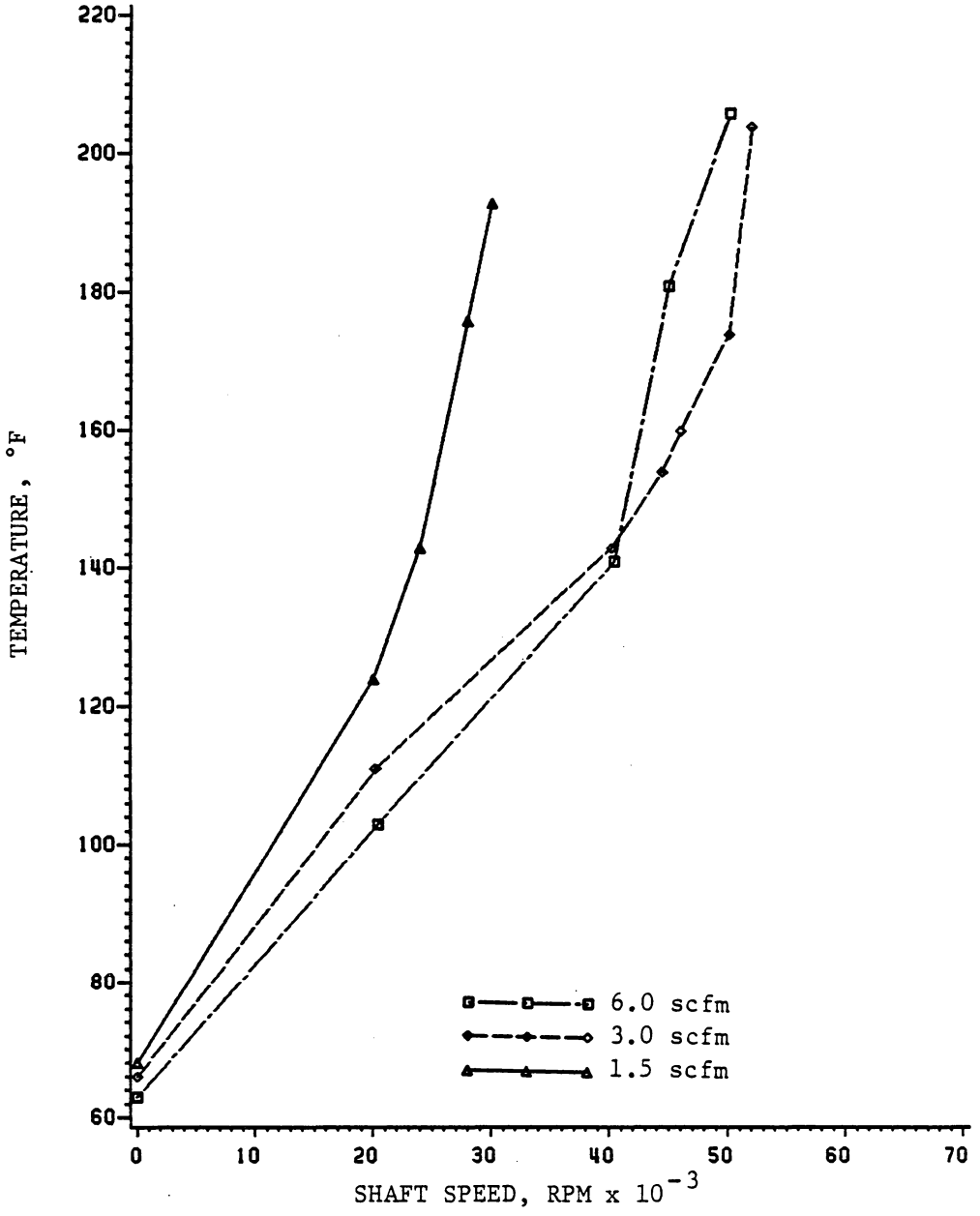

Fig. 15. Test Results for the Angular Contact Bearing with a 100 lb Thrust Load.

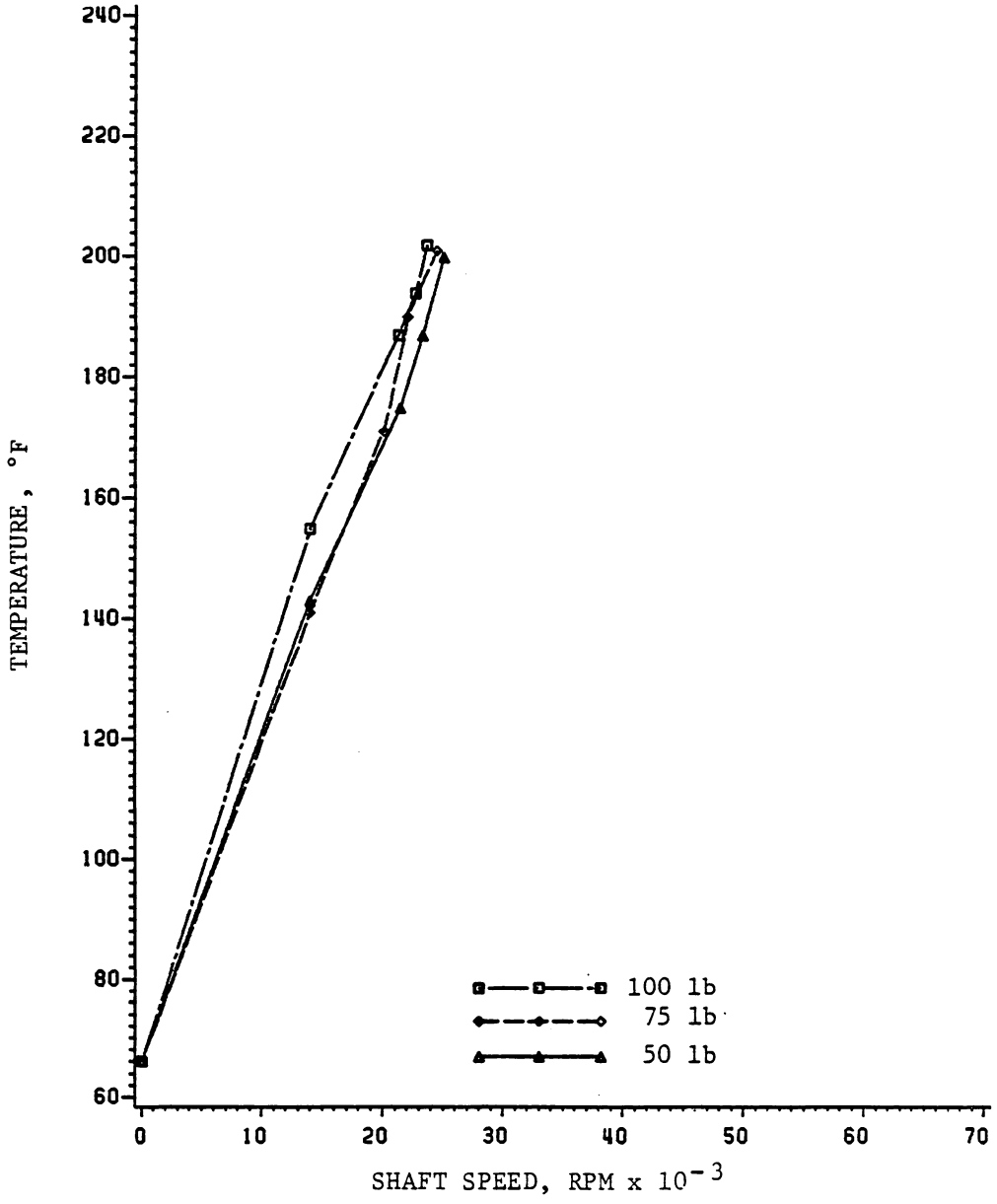

Fig. 16. Test Results for the 30mm Deep Groove Bearing with a 1.5 scfm Air Flow.

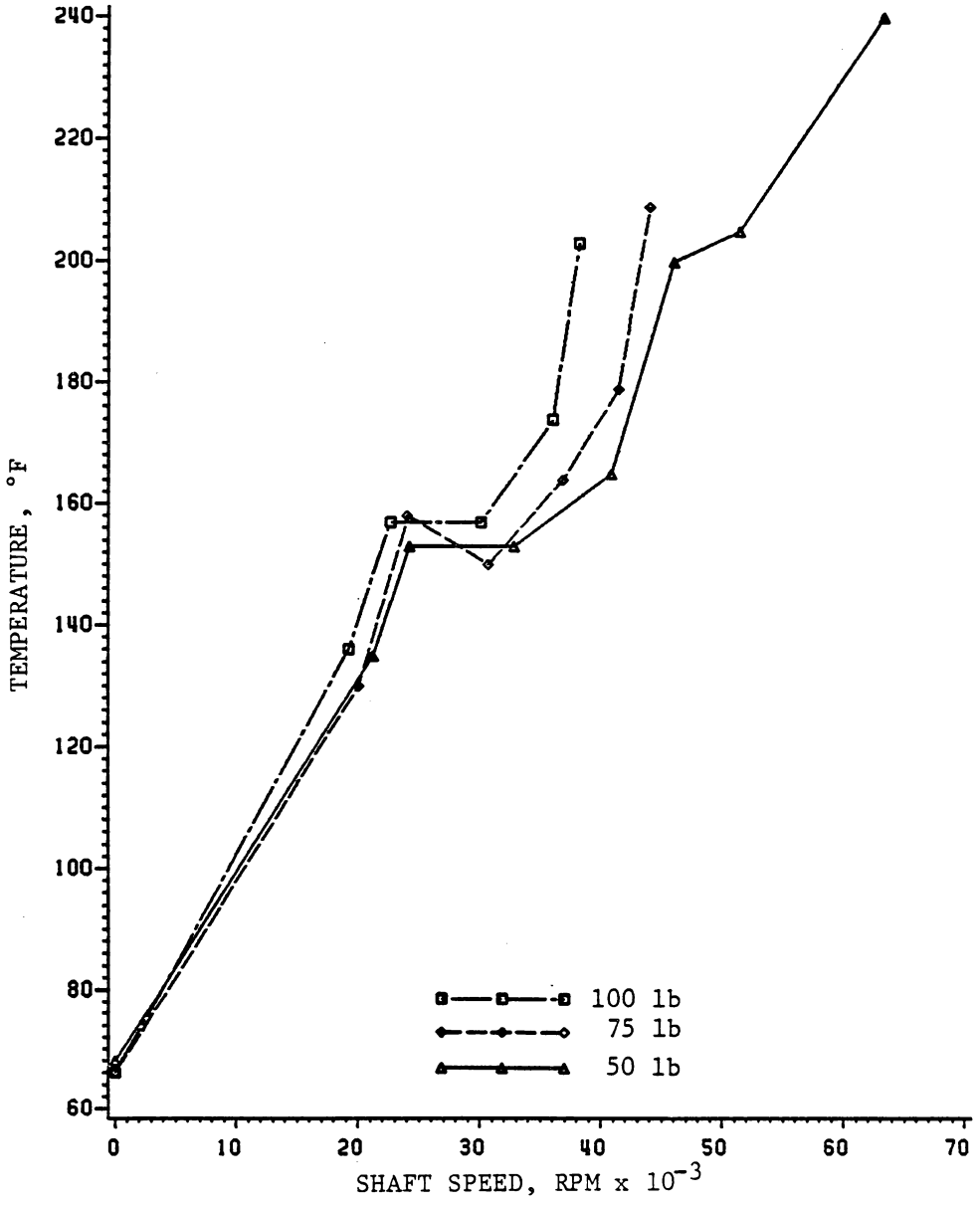

Fig. 17. Test Results for the 30mm Deep Groove Bearing with a 3.0 scfm Air Flow.

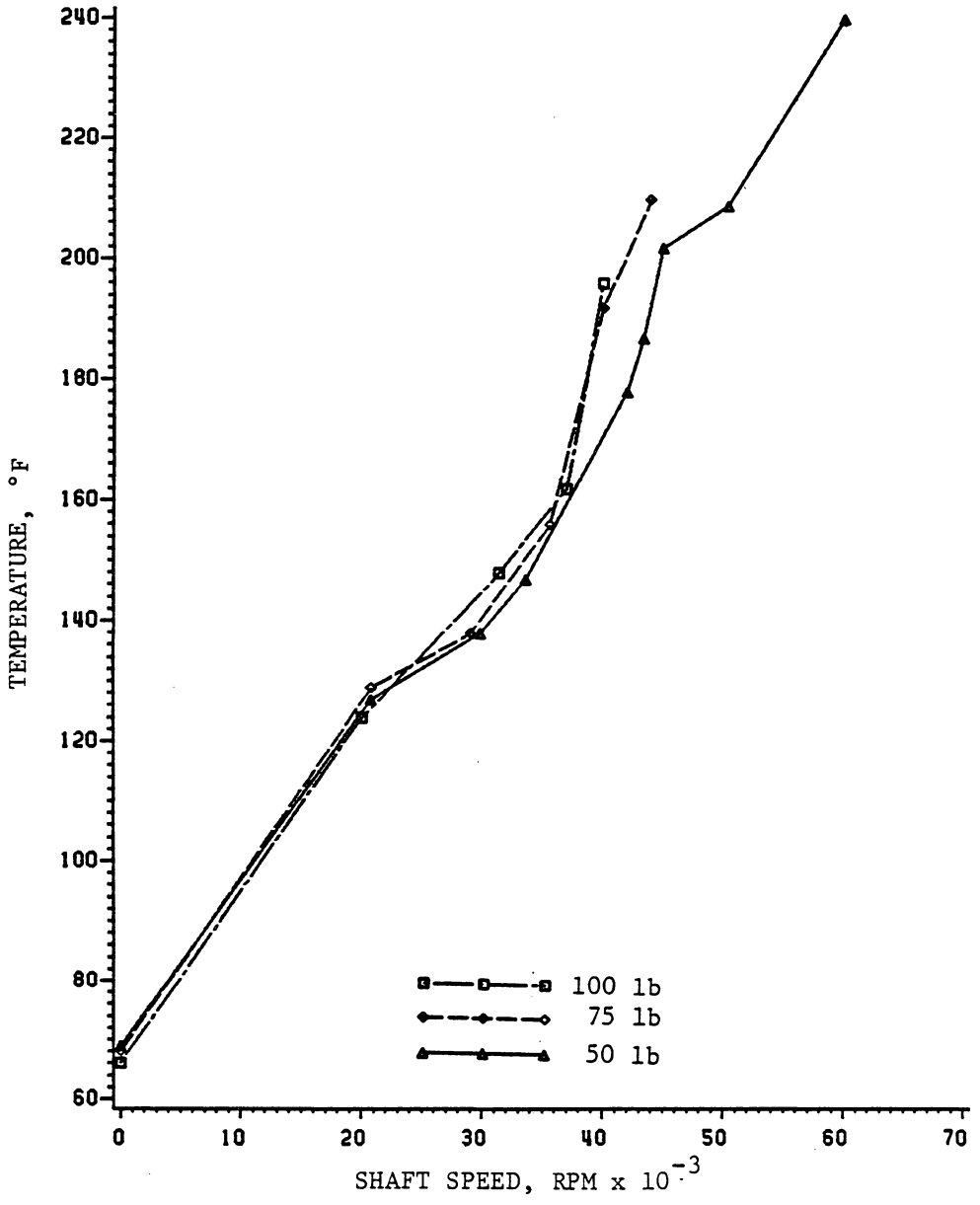

Fig. 18. Test Results for the 30mm Deep Groove Bearing with 6.0 scfm Air Flow.

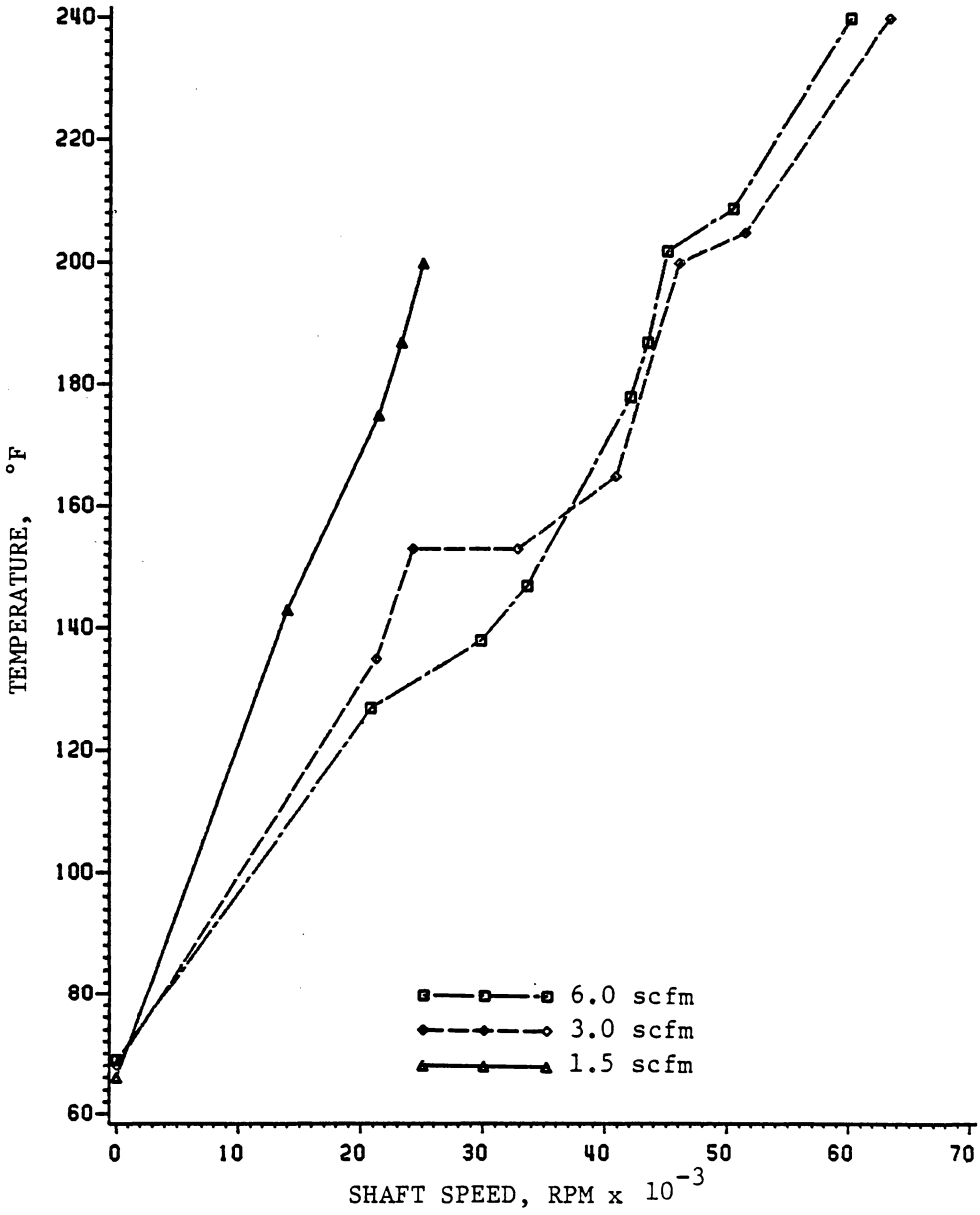

Fig. 19. Test Results for the 30mm Deep Groove Bearing with a 50 lb Thrust Load.

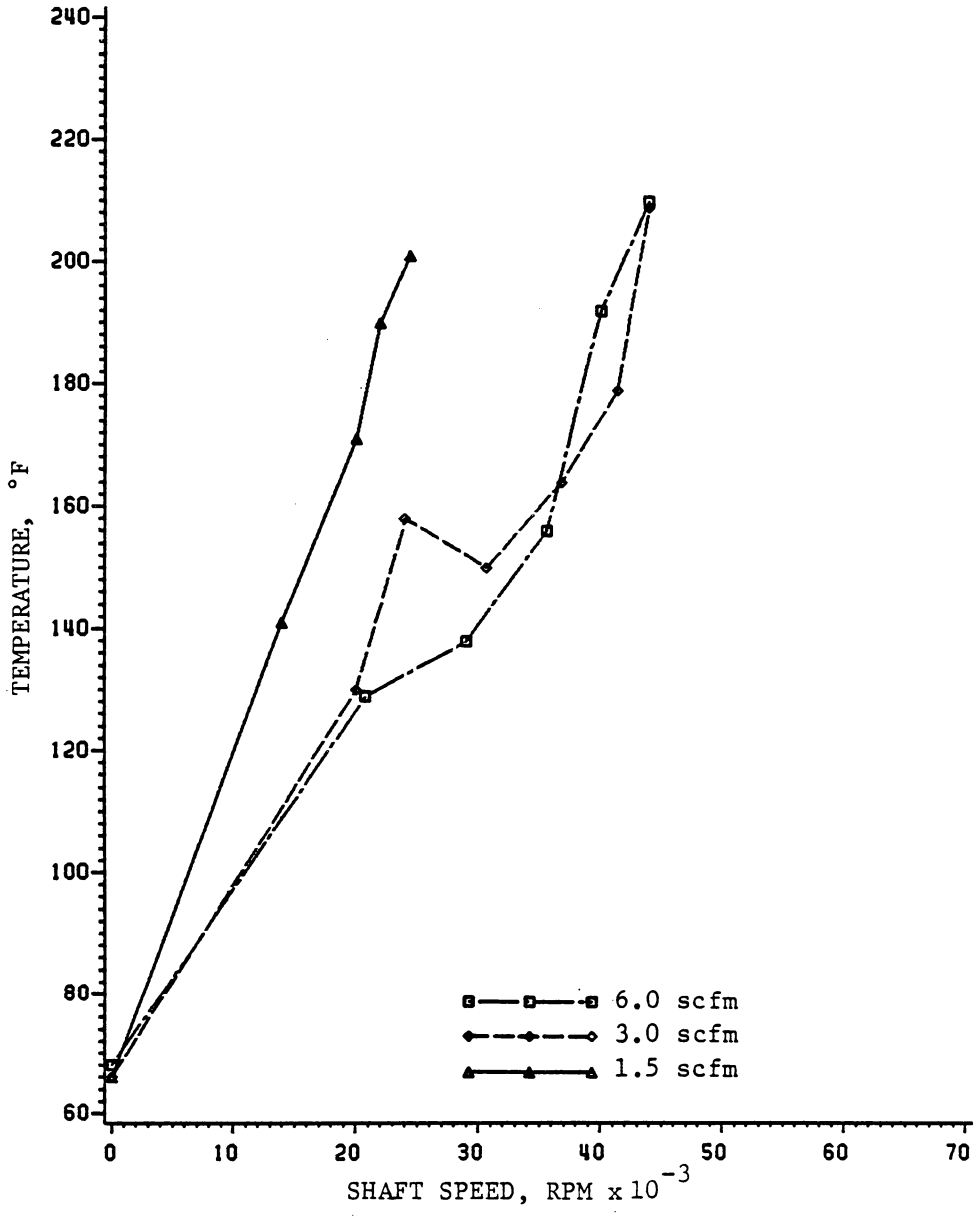

Fig. 20. Test Results for the 30mm Deep Groove Bearing with a 75 lb Thrust Load.

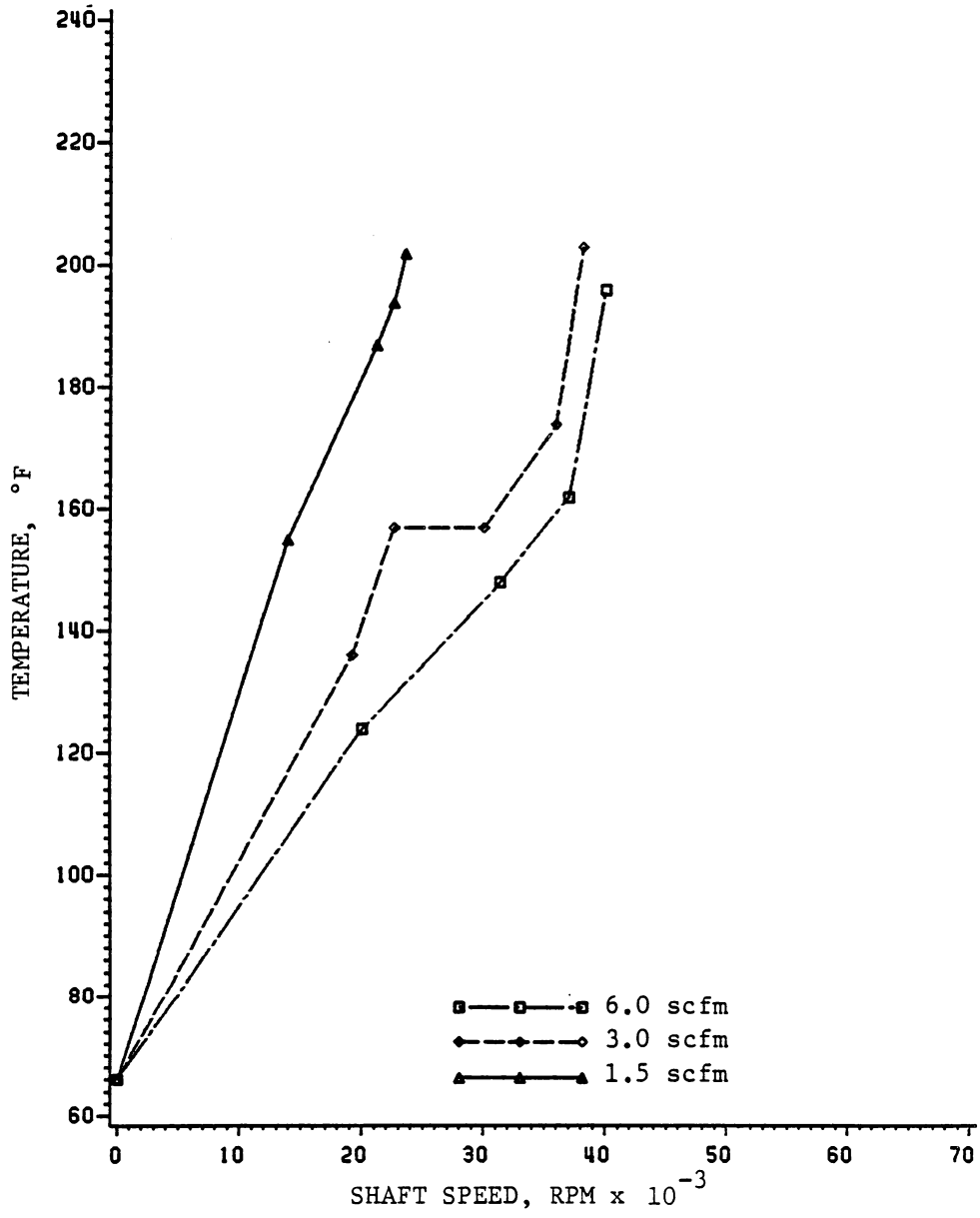

Fig. 21. Test Results for the 30mm Deep Groove Bearing with a 100 lb Thrust Load.

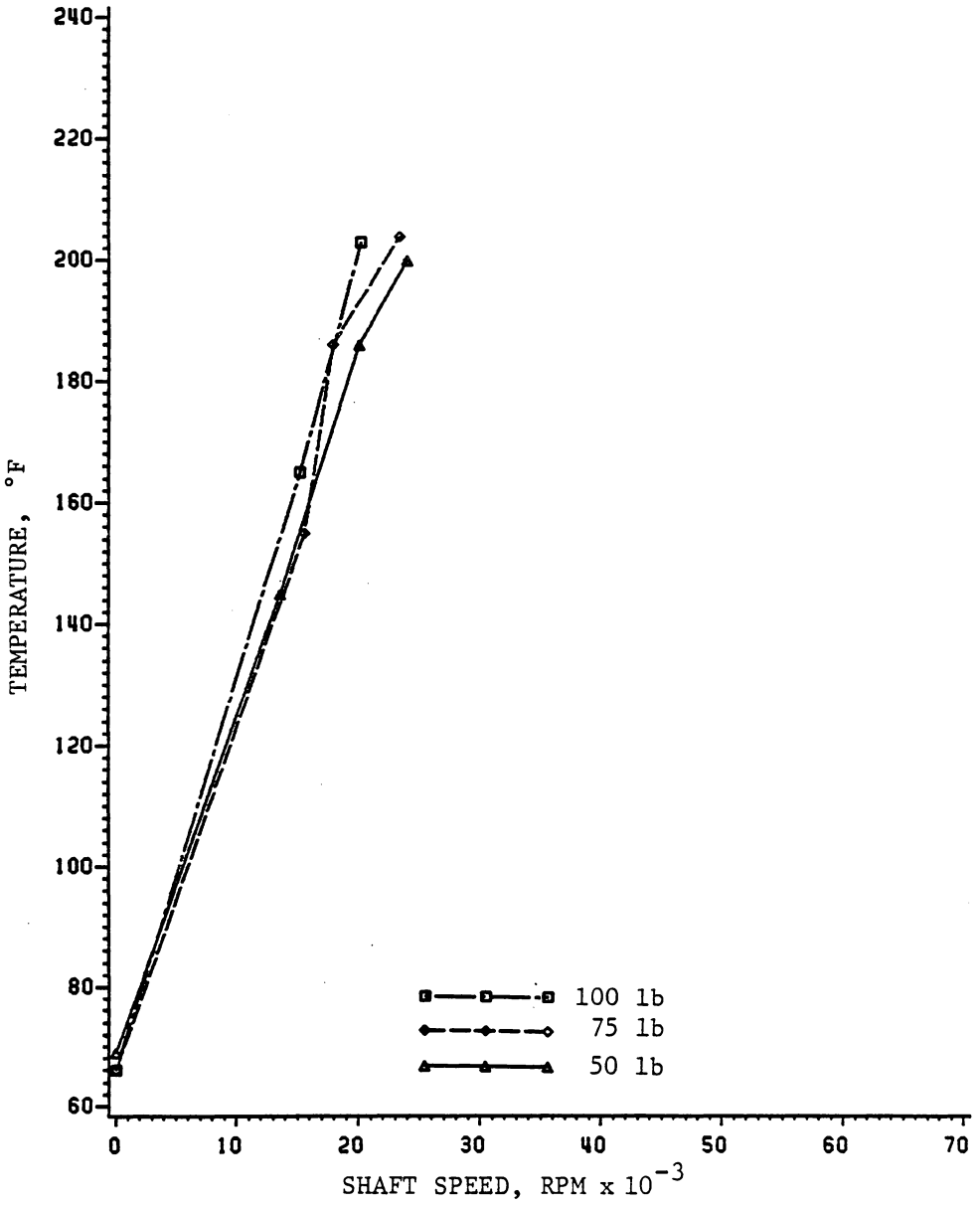

Fig. 22. Test Results for the 30mm Angular Contact Bearing with a 1.5 scfm Air Flow.

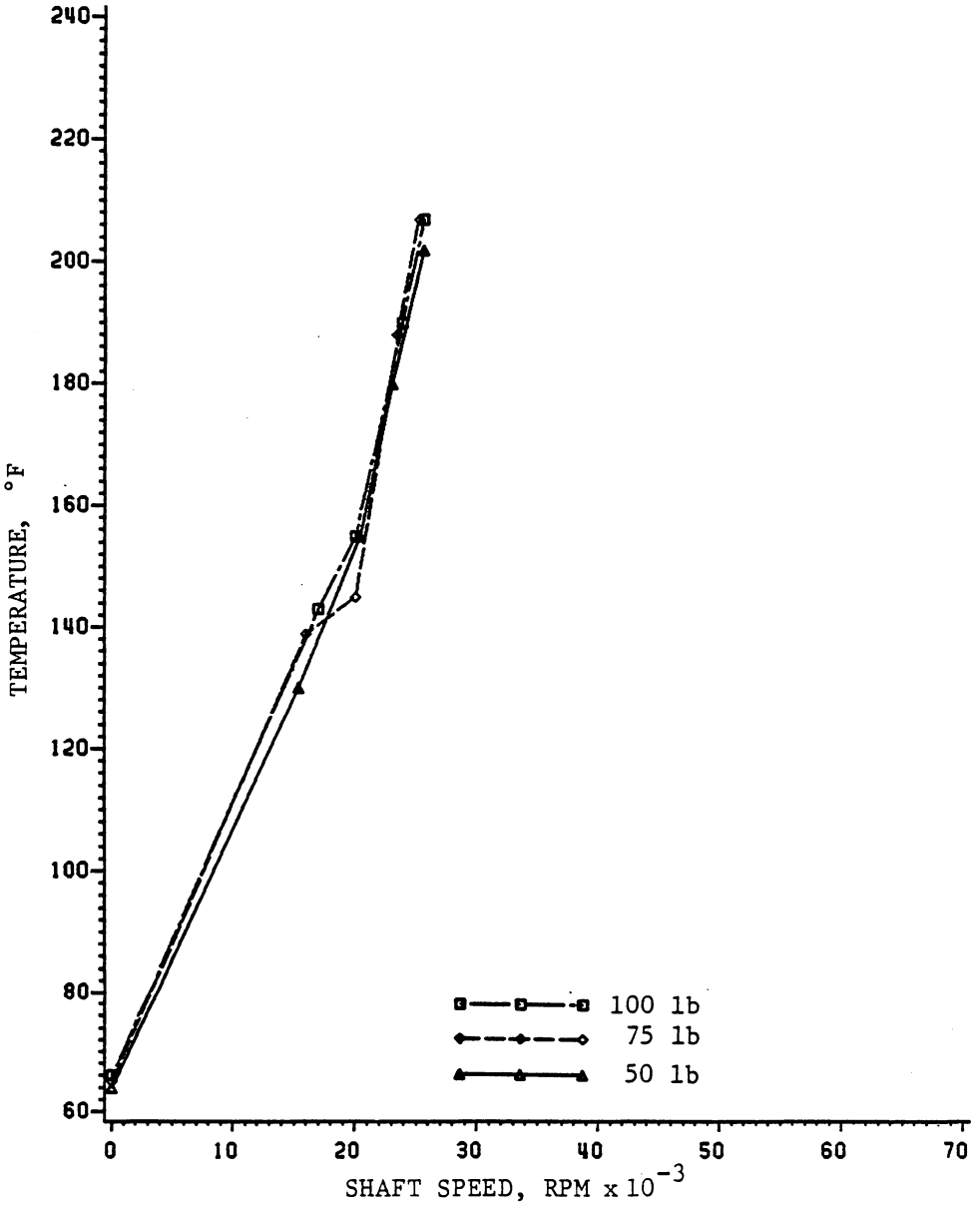

Fig. 23. Test Results for the 30mm Angular Contact Bearing with a 3.0 scfm Air flow.

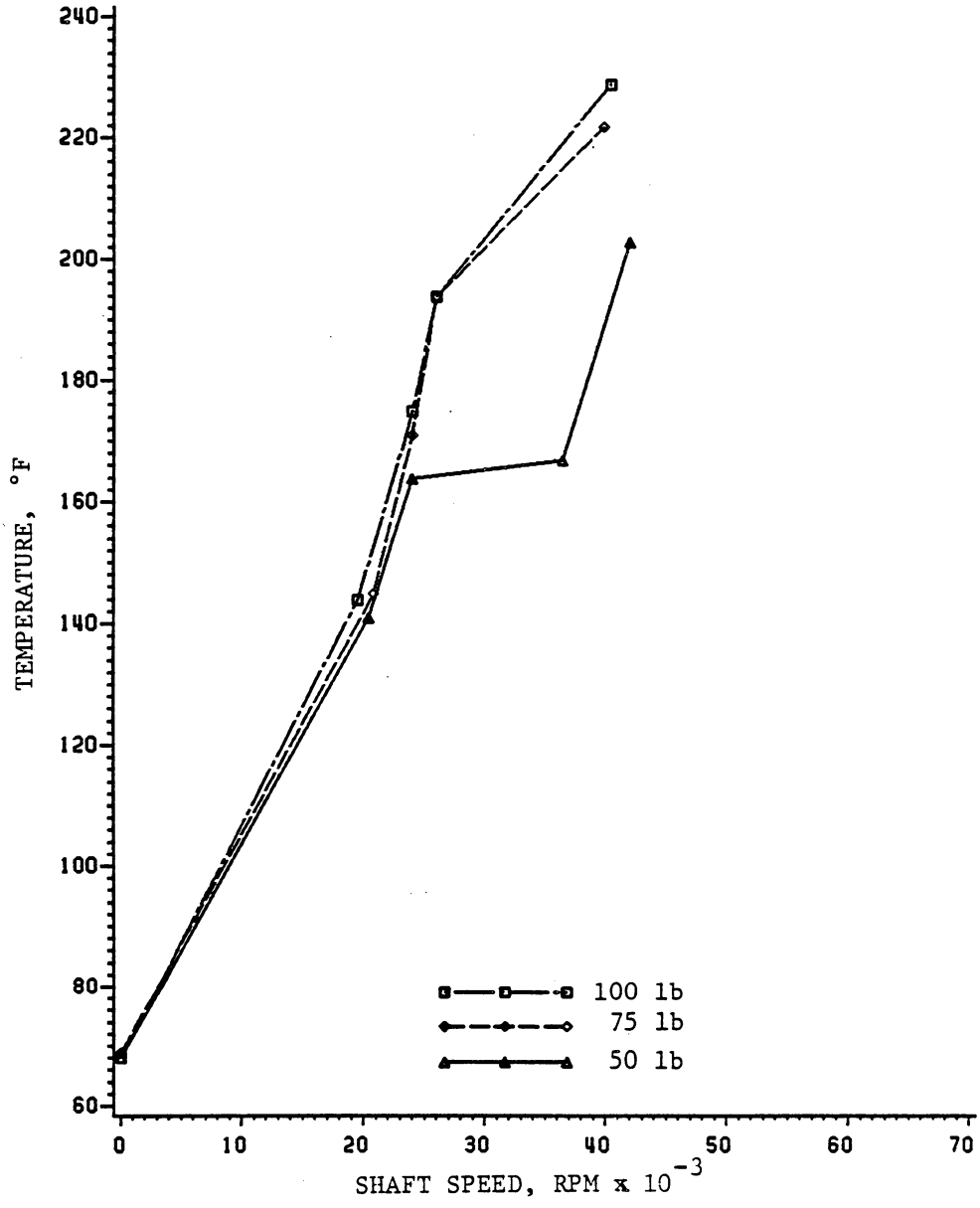

Fig. 24. Test Results for the 30mm Angular Contact Bearing with a 6.0 scfm Air Flow.

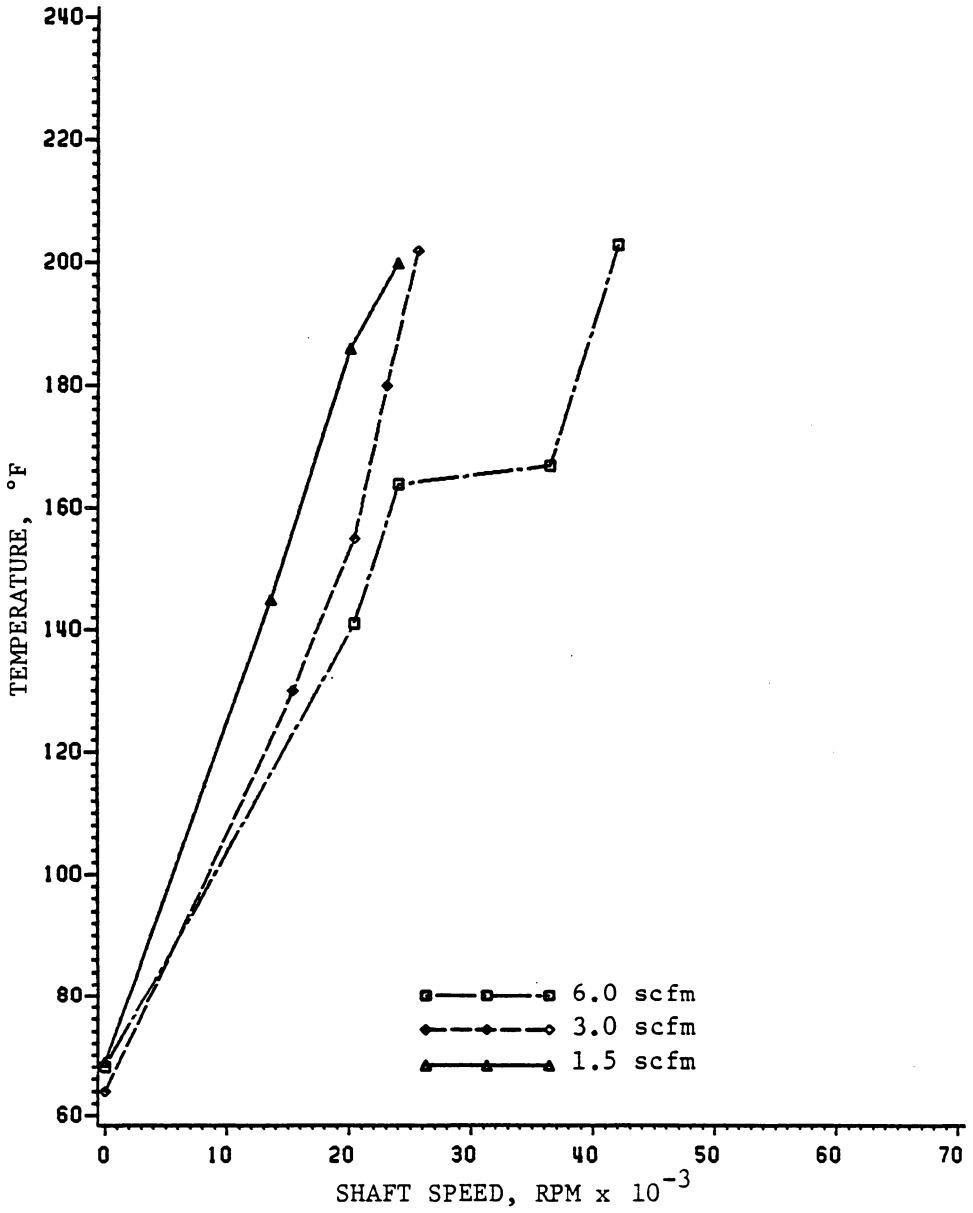

Fig. 25. Test Results for the 30mm Angular Contact Bearing with a 50 lb Thrust Load.

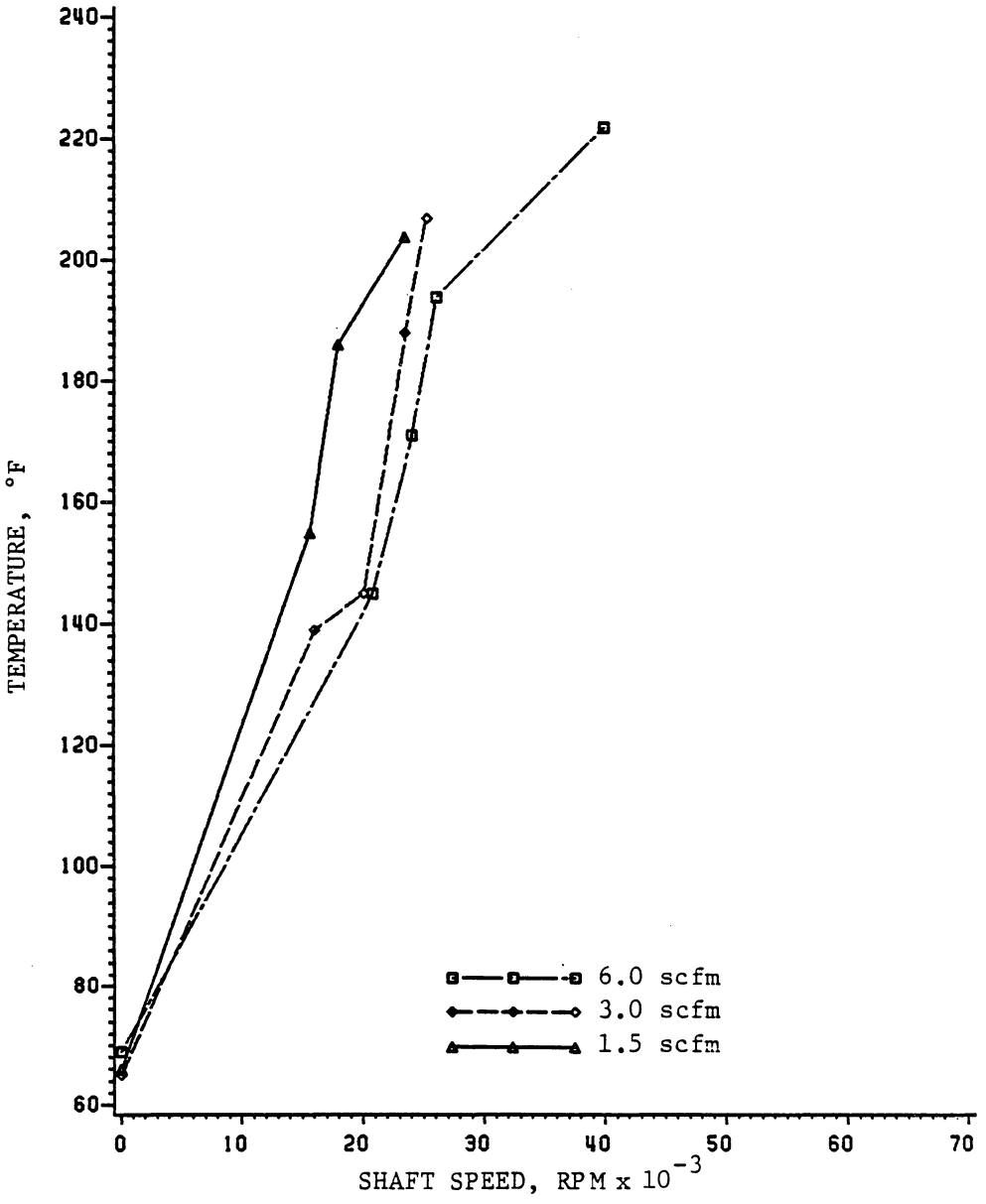

Fig. 26. Test Results for the 30mm Angular Contact Bearing with a 75 lb Thrust Load.

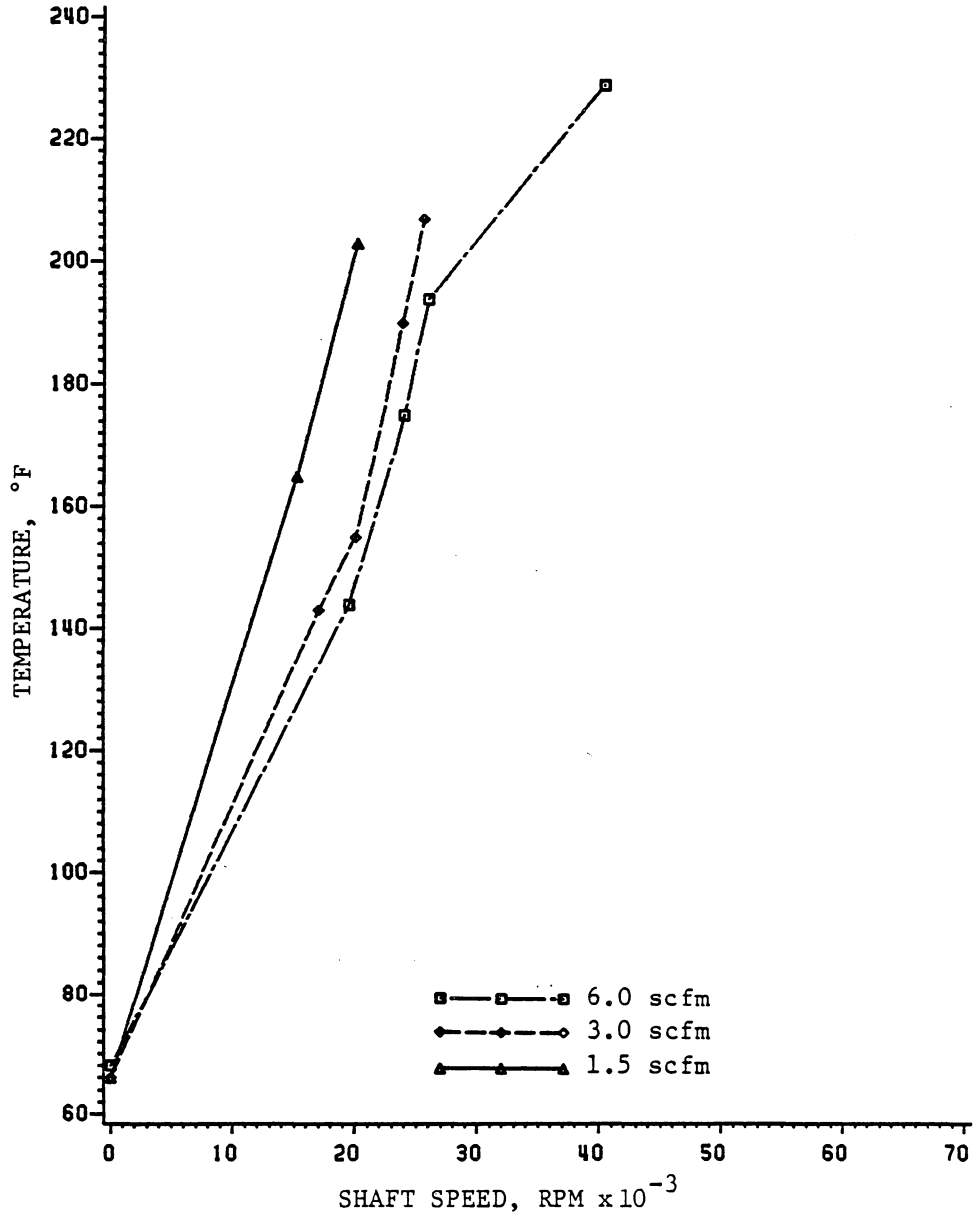

Fig. 27. Test Results for the 30mm Angular Contact Bearing with a 100 lb Thrust Load.

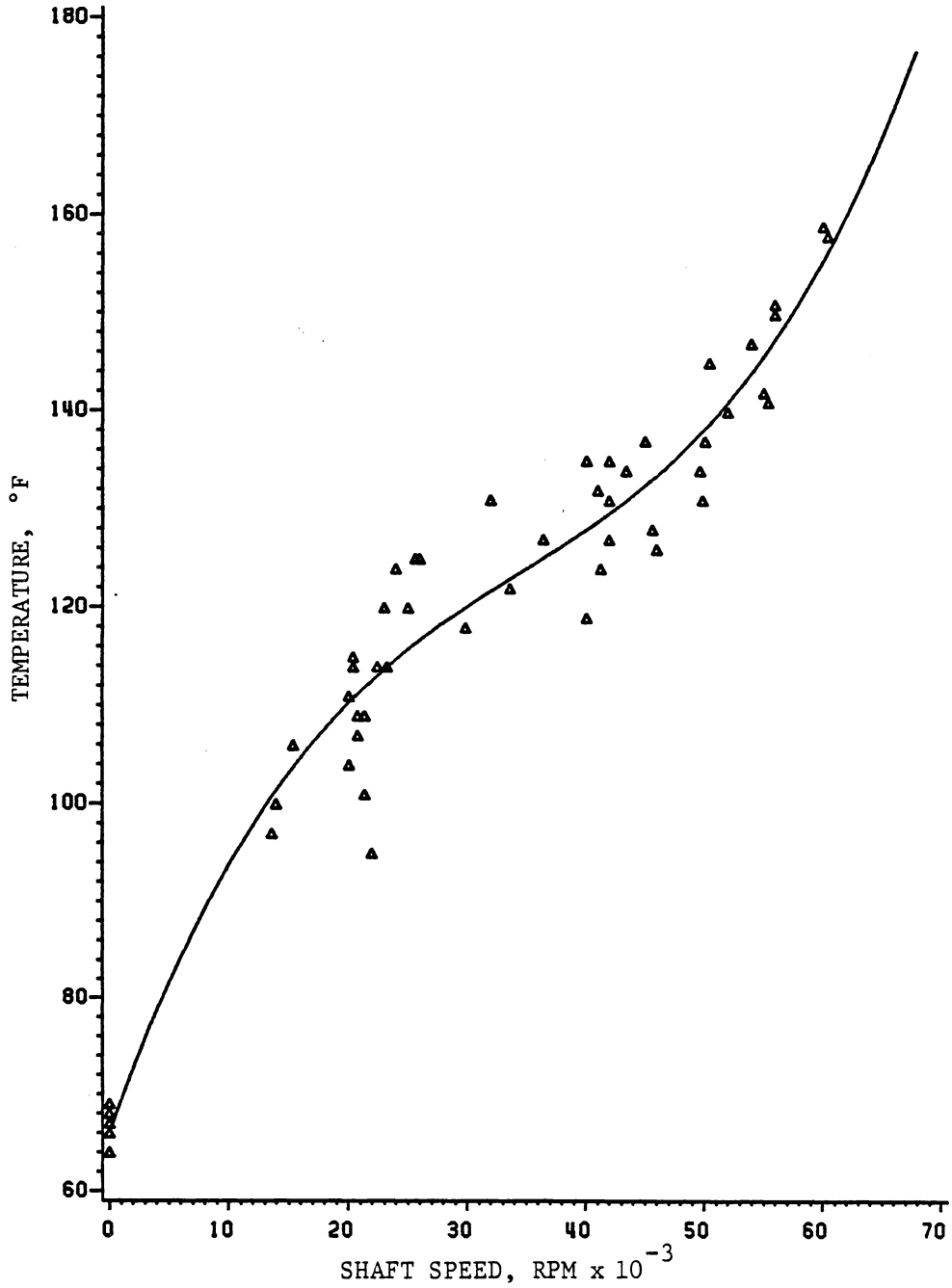

Fig. 28. Test Results for the 17mm Deep Groove Support Bearing with a 71 lb Thrust Load and 13 lb Radial Load.

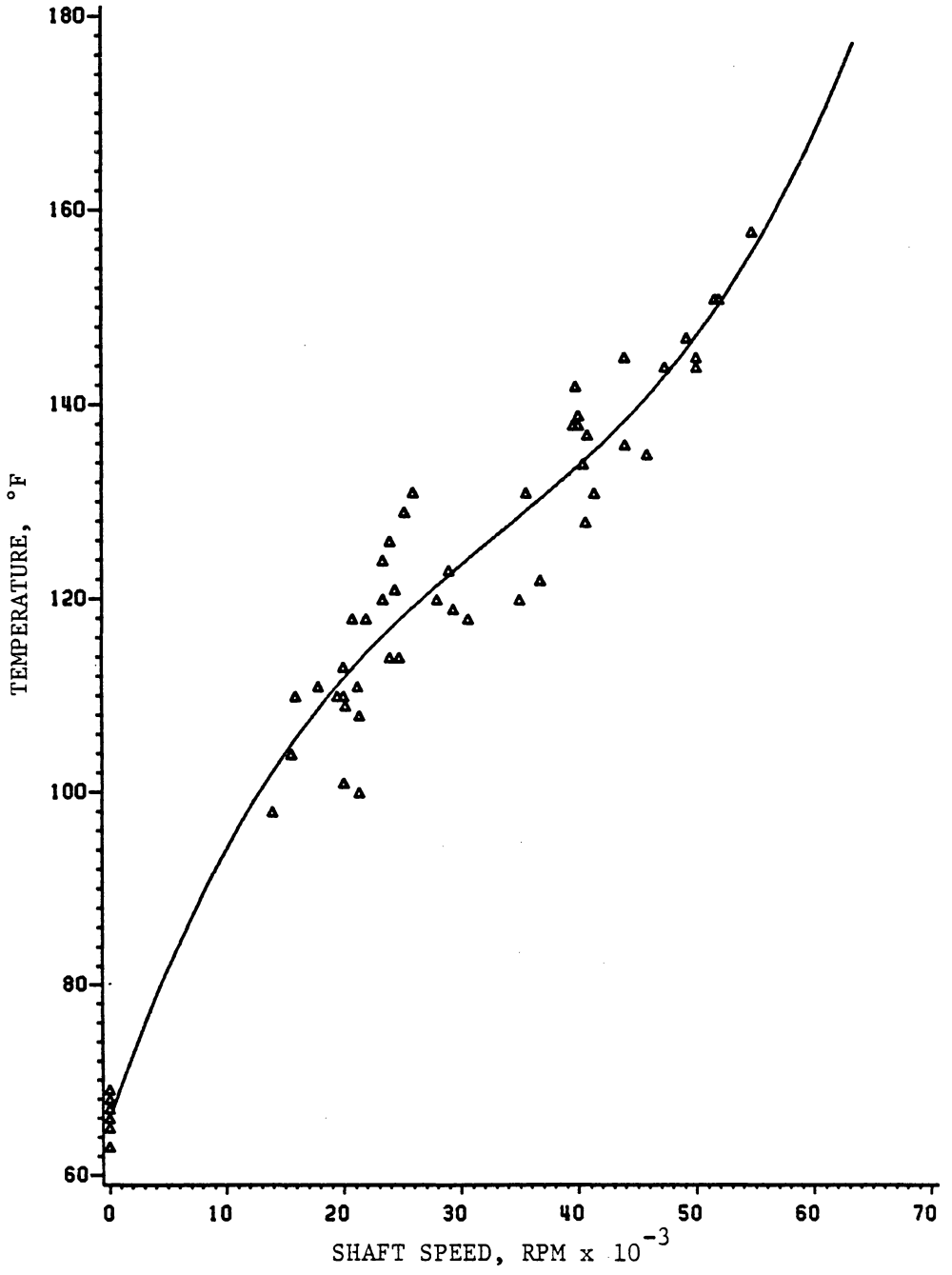

Fig. 29. Test Results for the 17mm Deep Groove Support Bearing with a 96 lb Thrust Load and 13 lb Radial Load.

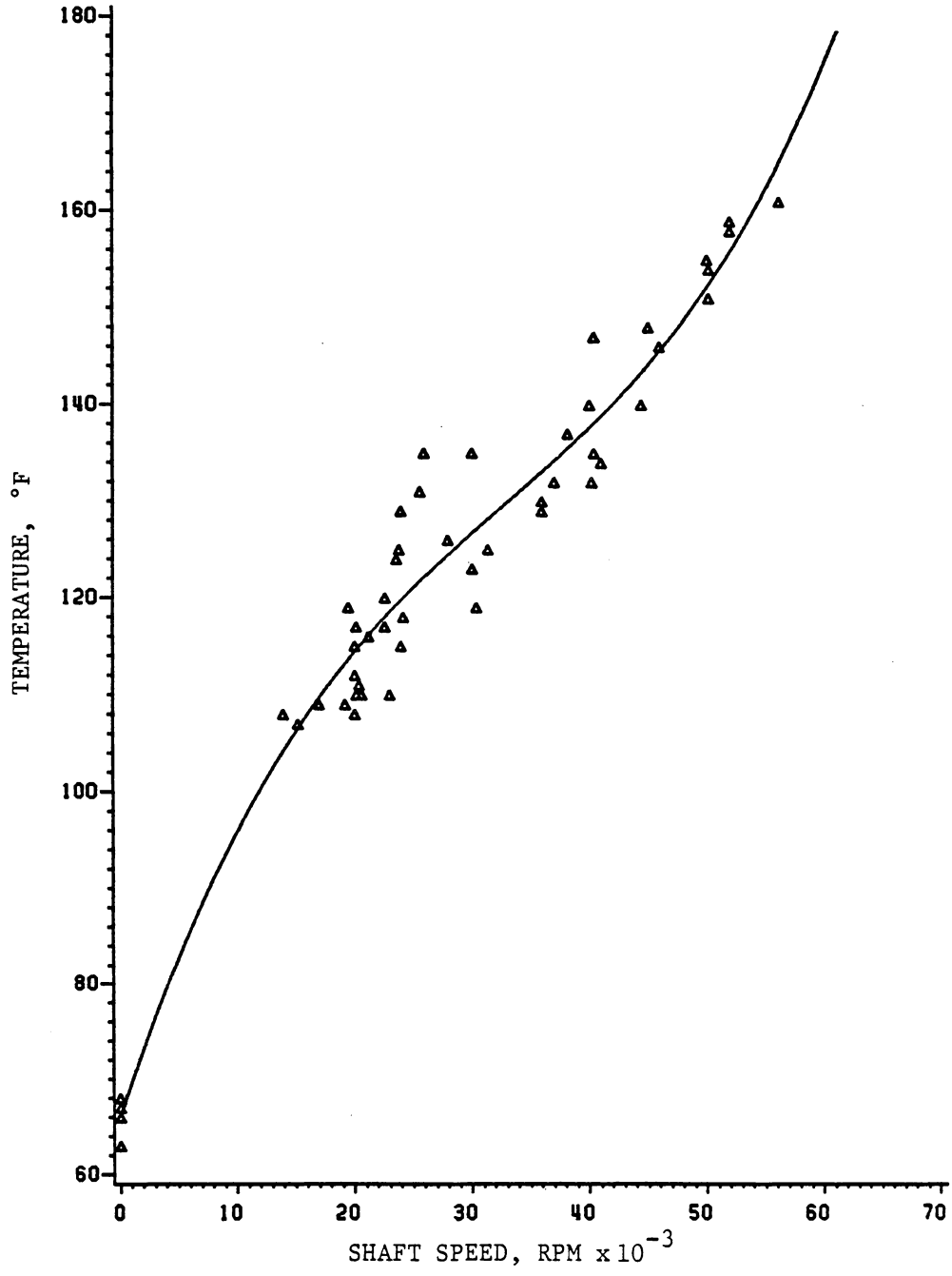

Fig. 30. Test Results for the 17mm Deep Groove Support Bearing with a 121 lb Thrust Load and 13 lb Radial Load.

V. ANALYSIS OF RESULTS

The results presented in the previous chapter represent 200 test bearing temperature observations at different load, air-oil mist flow, and speed conditions. In order to establish relationships between these variables, a multiple linear regression analysis was performed on the data sets corresponding to each of the four test bearings. The result of this analysis is an equation for each test bearing that can, within certain constraints, be used to estimate bearing outer race temperature under various conditions. No analysis was performed on the 17 mm support bearings. Since the air-oil mist flow was not varied, only slight temperature variation with load was observed, and these bearings were always operated below 1.2 times the catalog limiting speed, an analysis would yield little additional information over the graphical results presented in the previous chapter.

In this chapter, a brief description of the multiple regression analysis technique is presented, followed by details of the analysis procedure as applied to the present research. The equations resulting from this analysis are then presented with their estimated limiting speed. Finally, selected comparisons are made between predicted and actual results.

Regression analysis is a statistical technique for investigating and modeling the relationship between variables [14]. Multiple linear regression involves one dependent or response variable, y, and more than one independent or regressor variable as in the equation below.

$$y = \beta_o + \beta_1 x_1 + \beta_2 x_2 + \beta_3 x_3 + \ldots . \beta_n x_n + \varepsilon$$

Given a specific set of m observations,

$$(y_1, x_{11}, x_{21}, x_{31} \cdots x_{n1}) \text{ to } (y_m, x_{1m}, x_{2m}, x_{3m} \cdots x_{nm}) ,$$

the purpose of the regression analysis is to estimate the unknown coefficients $\beta_o, \beta_1 \cdots \beta_n$. The error between the estimated value of y and the true value is ε. In general, higher order effects and interaction effects in the independent variables can be modeled as in the example below:

$$y = \beta_o + \beta_1 x_1 + \beta_2 x_1^2 + \beta_3 x_1 x_2 + \cdots + \varepsilon$$

Although this model is nonlinear in the regressor variables, it is linear in the coefficients, $\beta_o \cdots \beta_n$. The multiple linear regression analysis is equally applicable to such a model.

The first step (after data collection) of the present analysis was to establish suitable regressor variables to describe the data. It is generally desirable to keep the model simple without omitting significant variables [14]. The initially chosen variables and their units are given below:

DN - bearing bore x speed, mm • x (RPM x 10^{-3})
DN^2 - bearing bore x $speed^2$, mm • x (RPM x $10^{-3})^2$
DN^3 - bearing bore x $speed^3$, mm • x (RPM x $10^{-3})^3$
AF - air flow, scfm
OF - oil flow, ml/min
L - load, lb

The response variable, ΔT, was taken as the temperature difference in degrees Fahrenheit between the bearing outer race temperature and the cooling air inlet temperature. This was done to account for slight variations in the inlet air temperature for different test runs, and to make the resulting prediction model more general. With the above selection of response and regressor variables, the general model appears as shown below:

$$\Delta T = \beta_1(DN) + \beta_2(DN^2) + \beta_3(DN^3) + \beta_4(AF) + \beta_5(OF) + \beta_6(L)$$

The quadratic and cubic speed terms were included to allow for nonlinear temperature variation with speed.

With the general model defined, the possibility of an improved model based on a subset of the general model regressor varibles was investigated. Using a computer analysis routine [15], each regressor and combination of regressor variables were systematically eliminated from the general model to determine if a better model existed. This model selection process was done for each of the four test bearings. The "best" model was chosen based on the minimum value of the PRESS statistic. Since PRESS is defined as the "sum of squared differences between the observed and predicted value of the response variable" [14], a minimum value of PRESS indicates a model that predicts well within the range of the observed responses.

The prediction equations resulting from this analysis are given in Fig. 31* with the applicable maximum speed corresponding to each equation clearly stated. It is important to note that these equations should not be used for extrapolation outside the range of the original data. Furthermore, making inferences based on the regressor variable coefficients can be misleading. These coefficients may, in fact, be poor estimates of the true unknown coefficients, but the model still provides a good prediction equation over the data range (14).

A comparison between the regression model prediction equations and the actual test data for each test bearing at a 3.0 scfm (0.10 kg/min) air flow and a 75 pound (334 N) thrust load is shown in Figs. 32 through 35. The equation for the 25 mm deep groove bearing does an excellent job of predicting the actual bearing temperature as shown in Fig. 32. In Fig. 33, for the 25 mm angular contact bearing, the equation again does a good job of predicting temperature. In both of these figures the prediction curves show temperatures that rise rapidly at higher speeds as generally expected and observed.

In Fig. 34, for the 30 mm deep groove bearing, the regression equation predicts the temperatures fairly well, but the curve shows a decreasing rate of temperature rise due to the negative coefficient on DN^2 that does not seem intuitively correct. Figure 35 for the 30 mm angular contact bearing shows good temperature prediction at lower speeds. But between 35,000 and 40,000 RPM, the regression equation

---

*The coefficients in the equations of Fig. 31 have been rounded off for clarity of presentation. The reader is referred to Appendix B for the full coefficients that should be used in calculations.

predicts virtually no increase in temperature. Above 40,000 RPM (not shown) the predicted temperature actually decreases rapidly due to the negative coefficient on the DN^3 variable. It is apparent that the equation cannot be used to extrapolate temperature predictions.

The reader is referred to Appendix B for specific statistics on the four prediction equations resulting from this analysis.

25mm Deep Groove 60,000 RPM Maximum

$$\Delta T = 0.15\ DN - 2.79 \times 10^{-3}\ DN^2 + 3.36 \times 10^{-5}\ DN^3 - 11.94\ AF + 342.0\ OF + 0.27\ L$$

25mm Angular Contact 56,000 RPM Maximum

$$\Delta T = 0.082\ DN + 8.37 \times 10^{-6}\ DN^3 - 23.8\ AF + 1035\ OF + 0.127\ L$$

30mm Deep Groove 63,000 RPM Maximum

$$\Delta T = 0.135\ DN - 5.9 \times 10^{-4}\ DN^2 - 24.5\ AF + 939\ OF + 0.246\ L$$

30mm Angular Contact 40,000 RPM Maximum

$$\Delta T = 0.092\ DN + 6.48 \times 10^{-3}\ DN^2 - 1.37 \times 10^{-4}\ DN^3 - 10.7\ AF + 247.8\ OF + 0.246\ L$$

Figure 31. Test Bearing Temperature Prediction Equations

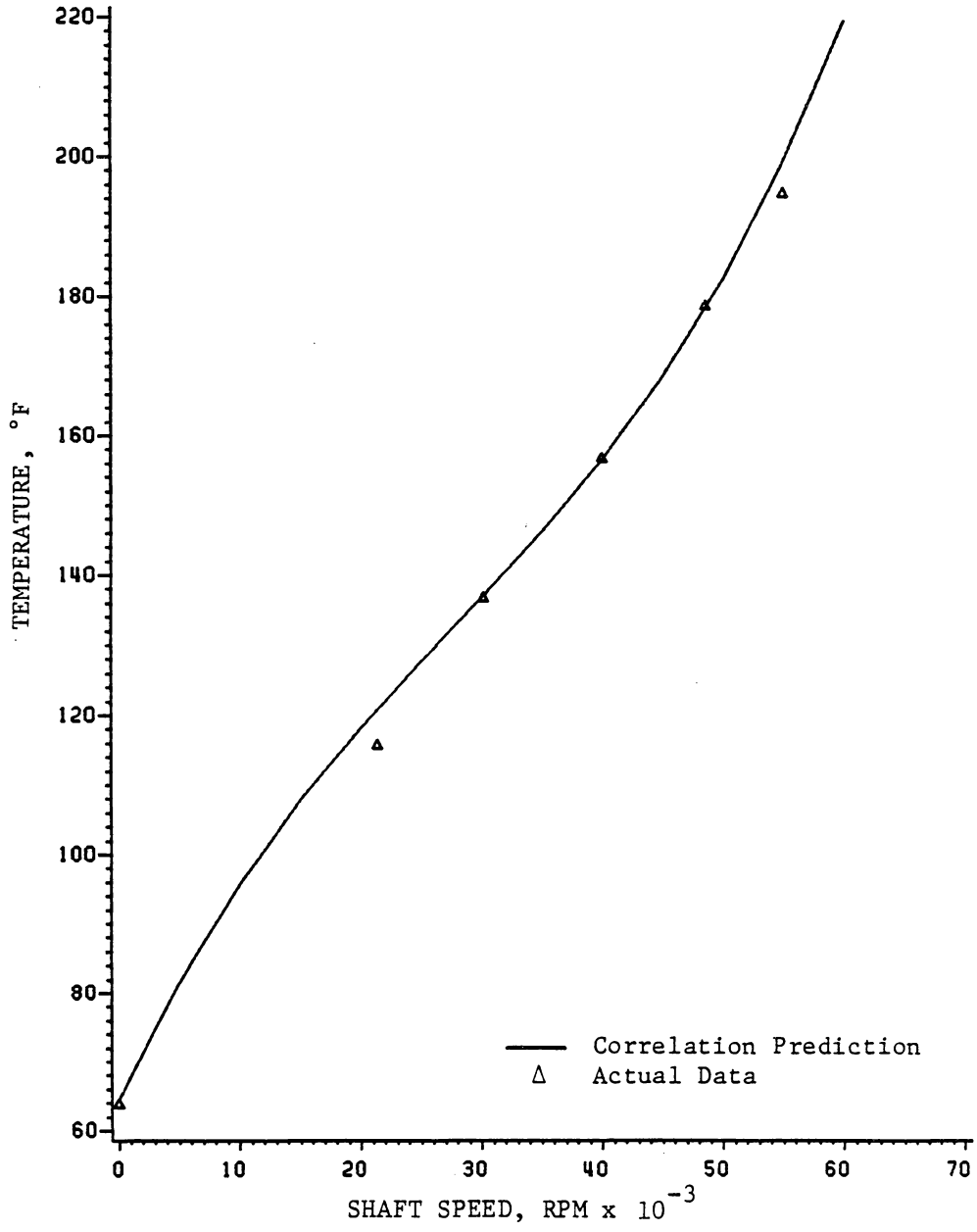

Fig. 32. Comparison of Correlation Prediction and Actual Results for the 25mm Deep Groove Bearing.

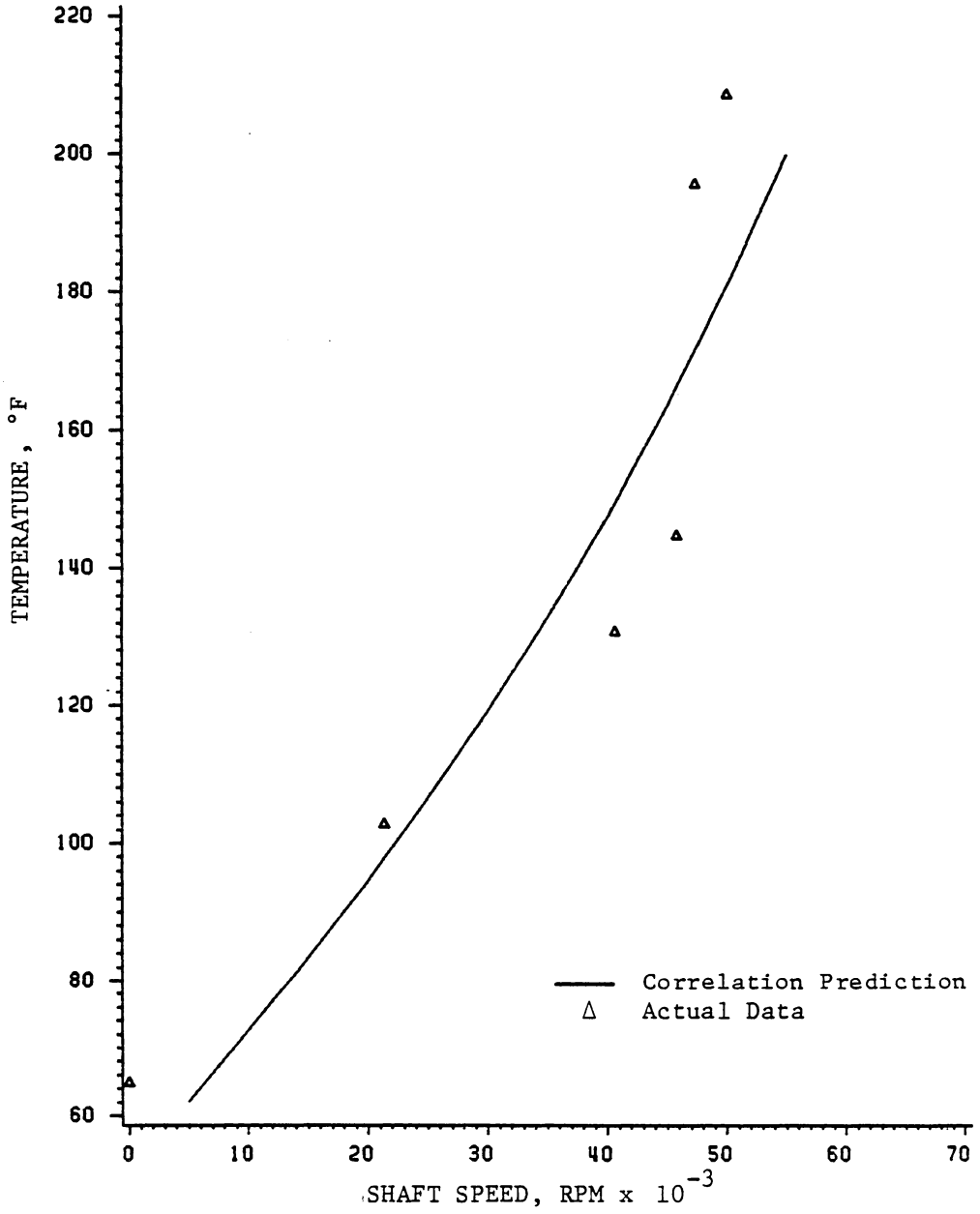

Fig. 33. Comparison of Correlation Prediction and Actual Results for the 25mm Angular Contact Bearing.

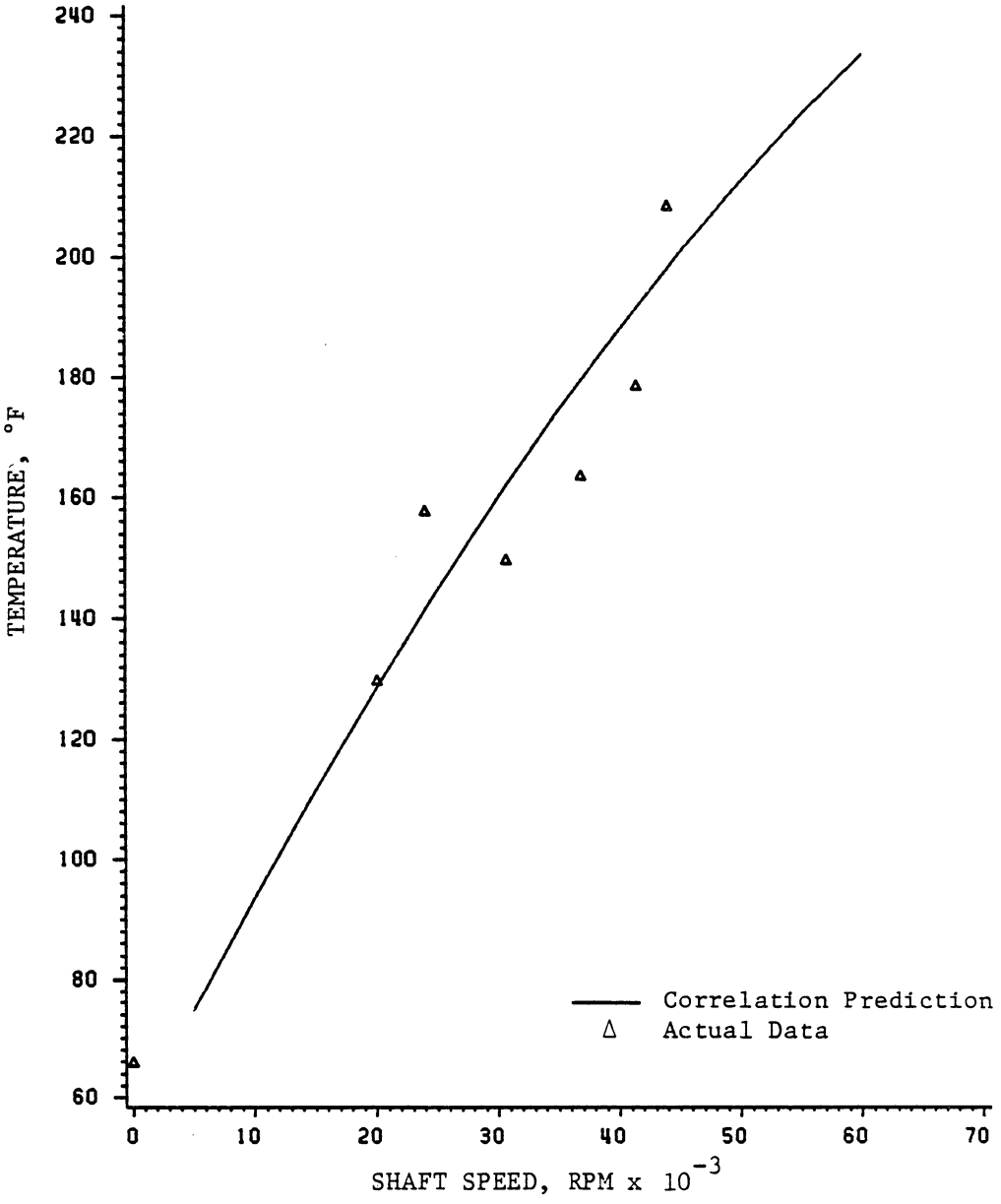

Fig. 34. Comparison of Correlation Prediction and Actual Results for the 30mm Deep Groove Bearing.

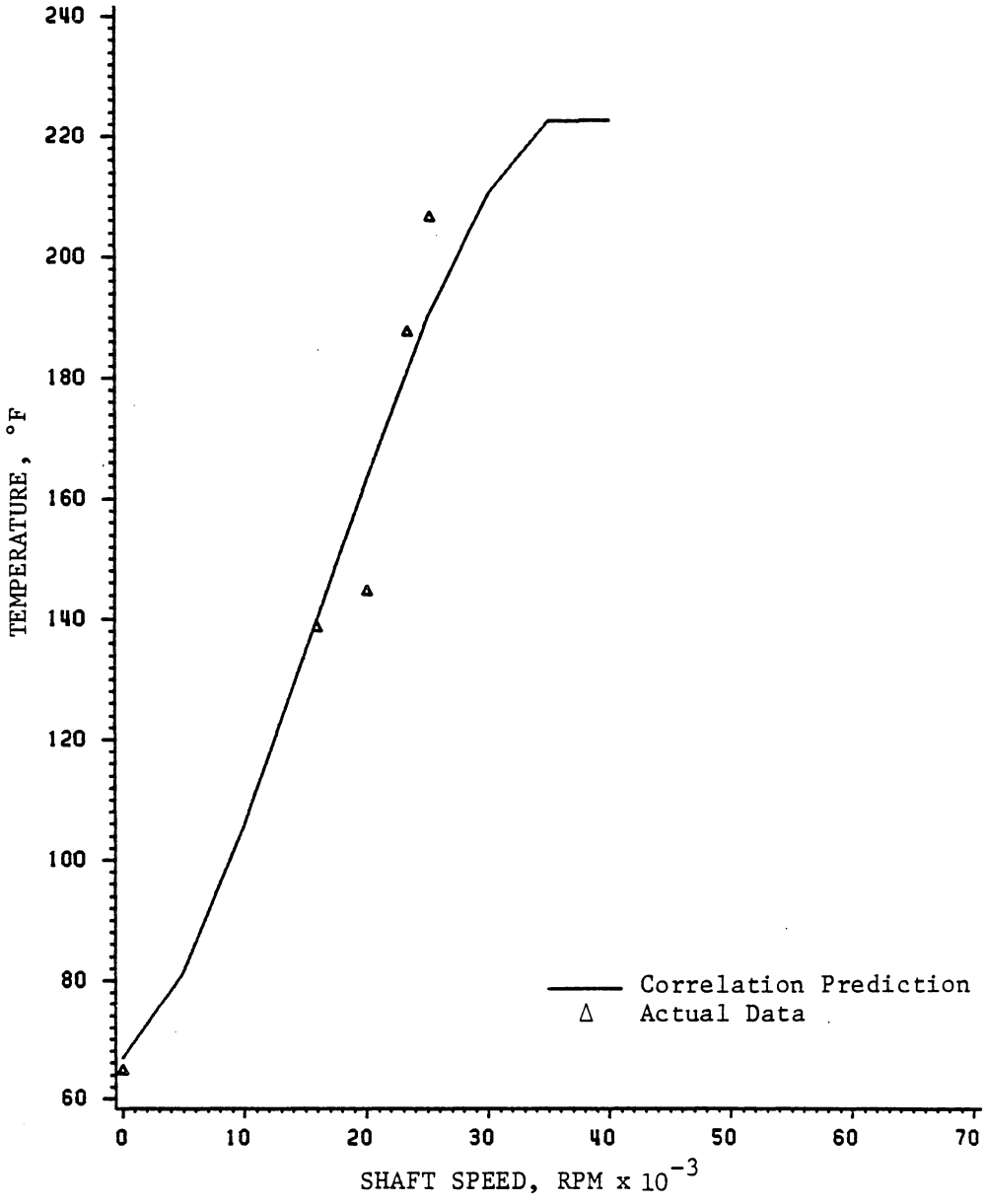

Fig. 35. Comparison of Correlation Prediction and Actual Results for the 30mm Angular Contact Bearing.

VI. DISCUSSION OF RESULTS

The highest operating speed was achieved with the 30mm deep groove bearing during a test rig performance run. The bearing was operated at 63,200 RPM (1.9×10^6 DN) with a stabilized outer race temperature of 240°F (389 K), an air flow of 3.0 scfm (0.10 kg/min), and a 50 pound (222 N) thrust load. This does not necessarily indicate that the 30mm deep groove bearing has a higher speed capability than the 25mm bearings. The 25mm test runs were usually terminated when the outer race temperature reached about 200°F (366 K) as explained in section 3.5. Still, it is surprising that the 30mm deep groove bearing could achieve a stable operating temperature at 1.9×10^6 DN, especially with only 3.0 scfm (0.10 kg/min) of cooling air, while the 25mm deep groove bearing had an outer race temperature of 208°F (371 K) at only 1.5×10^6 DN.

The apparent performance difference between the 25 and 30 mm deep groove bearings could possibly be due to a cage resonance or an instability in the 25mm bearing. A cage instability was observed at about 54,000 RPM during a very early preliminary run with a 25 mm deep groove bearing. During this particular run, the test bearing housing had a cover with large observation holes to allow a strobe light to be used to view the bearing while operating. The cage instability was very pronounced, and caused the cage to vibrate violently so that it appeared to blur under the strobe light. At speeds just below the instability, the cage appeared to operate very smoothly. It was possible to operate above the instability, but it is not certain whether the cage sustained any damage in going through the instability.

Referring to Fig. 6 for the 25mm deep groove bearing at 6.0 scfm (0.20 kg/min) air flow, it can be seen that a marked temperature rise occurs between 52,000 and 58,000 RPM for all three load conditions. For the 50 pound (222 N) load condition, the temperature rise between 56,000 and 60,400 RPM was not as high, but operation to 64,000 RPM (not shown in Fig. 6) resulted in a temperature rise to 230°F (383 K) that did not appear to be stabilizing. The rapid temperature rise between 52,000 and 58,000 RPM supports the earlier observation of a cage instability in this speed range, but if this were the only cause of the high temperatures, successful operation to speeds well above the instability might be expected. Since only one test run to a speed range above the region of cage instability was conducted, it is difficult to draw firm conclusions as to which deep groove bearing performed better.

If the temperature prediction equations resulting from the linear regression analysis are used to compare the 25 and 30mm deep groove bearings, the 30mm bearing has a higher predicted temperature at all air flow and load conditions up to 60,000 RPM. The equation for the 30mm bearing, however, predicts a decreasing rate of temperature rise while the 25mm bearing equation predicts an increasing rate of temperature rise at high speeds (see Fig. 31 and 33). Since these equations may not be good predictors of the true temperature response at data extremes or outside the data range, it is again difficult to draw firm conclusions on which bearing performed better at high speeds.

The angular contact bearings, in general, did not perform as well as the deep groove bearings. A maximum speed of 56,000 RPM (1.40×10^6 DN) was achieved with the 25mm bearing with a stable outer race

temperature of 208°F (371 K), while only 42,000 RPM (1.26×10^6 DN) was achieved with the 30mm bearing with an outer race temperature of 203°F (368 K). The cooling air flow was 6.0 scfm (0.20 kg/min) and the thrust load was 50 pounds (222 N) in both of these tests. The 30mm bearing was briefly operated to 46,000 RPM (1.38×10^6 DN), but the outer race temperature rose to 251°F (395 K) and did not stabilize so the test was terminated.

In Figs. 13, 14, and 15 for the 25mm angular contact bearing, it is apparent that a 1.5 scfm (0.05 kg/min) cooling air flow rate was not adequate for high speed operation. With the 30mm angular contact bearing, the temperature variation due to cooling air flow was much less pronounced than was observed for the 25mm bearings as shown in Figs. 25, 26, and 27. Temperature variation with load for the 30mm bearing was also not as significant (Figs. 22, 23, and 24). Considering the much higher temperatures observed for the 30mm angular contact bearing at any given speed, there must have been some significant influence on the bearing temperature other than cooling air flow rate or load. As mentioned previously, there were inconsistent test rig vibrations that may have influenced the bearing temperatures. During testing, the most difficulty due to rig vibrations occurred when running the 30mm angular contact bearing. The rig set-up was checked several times to insure proper bearing installation, alignment, and lubrication but no obvious cause for the vibration problems could be found. It is doubtful however, that the vibrations experienced could be the sole cause for the poor performance of the 30 mm angular contact bearing.

The temperature prediction equations were used to estimate the

speed of each test bearing corresponding to an outer race temperature of 200°F (366 K) and an incoming cooling air temperature of 70°F (294 K). A cooling air flow of 6.0 scfm (0.20 kg/min), an oil flow of 3.14×10^{-5} gal/min (0.120 kg/min), and a 50 pound (222 N) thrust load were used for this comparison. The results of this comparison are shown in Table 5.

For all tests conducted, the bearing temperature differences resulting from the 1.5 and 3.0 scfm (0.05 and 0.10 kg/min) air flows were higher than the bearing temperature differences for the 3.0 and 6.0 scfm (0.20 kg/min) flows. (The temperature difference was less pronounced with the 30mm angular contact bearing.) It appears that 1.5 scfm (0.05 kg/min) is simply not an adequate cooling air flow rate for high speed operation of 25 and 30mm ball bearings. Further, this indicates that a limiting condition might be reached such that little additional benefit is received from an increase in cooling air flow. This conclusion is supported by results cited in Chapter II (from Reference 11) where 1.8×10^6 DN was achieved with 7.5 scfm (0.25 kg/min), but a 90 scfm (3 kg/min) cooling air flow rate only extended operation to 2.16×10^6 DN. Based on the present research and Reference 11, air flows in the range of 6.0 to 9.0 scfm (0.20 to 0.30 kg/min) are approaching the limiting useful value for 25 to 30 mm bearings.

Temperature variation due to the different thrust loads was generally smaller than expected. Had a wider range of thrust loads been used, there probably would have been a more significant temperature variation with load. In high speed bearing operation a compromise must be made between increasing the thrust loads to prevent ball skidding, and reducing the load for longer bearing life.

Table. 5 Predicted Test Bearing Speeds for a 200°F Outer Race Temperature

25mm Deep Groove

58,000 RPM (1.5×10^6 DN)

25mm Angular Contact

53,500 RPM (1.34×10^6 DN)

30mm Deep Groove

47,500 RPM (1.43×10^6 DN)

30mm Angular Contact

31,500 RPM (0.95×10^6 DN)

At this point little has been said of the oil flows used during testing. In fact, the oil flow is probably the most difficult variable to control in an air-oil mist system. The small oil flow rates used can easily be upset by excessive "plating out" of oil particles in the distribution lines. If oil levels build up in lines, sudden surges in oil flow can result. In the present research, no attempt was made to establish a minimum oil flow requirement. No test bearing failures were encountered due to lack of lubrication, and visual inspection of the bearings revealed no excessive cage wear as might be expected if there were an inadequate supply of oil to the bearing. One of the 17mm support bearings did seize during an early test run, probably due to a lack of lubrication. During that particular run, the support bearing air flow had been reduced to approximately 0.5 scfm (0.017 kg/min) and the oil drip rate reduced to 20 drops/min per bearing. Bearing seizure occurred at 52,000 RPM. After this incident, the air flow was increased to 0.75 scfm (0.025 kg/min), and the oil flow increased to 30 drops/min per bearing. No further difficulty was encountered with the support bearings. In general, excessive oil to a bearing will result in higher bearing temperatures due to lubricant churning action. The positive coefficient on the oil flow term of the temperature prediction equations confirm this, but some minimum oil flow is obviously required.

Although the test bearing torque measuring system was never made operational, an estimate of the bearing power loss can be made based on the heat transfer to the cooling air. Since there was little heat loss through conduction because of the overhung housing, virtually all bearing generated heat had to be removed by the cooling air stream.

Using the First Law of Thermodynamics,

$$\dot{Q} = \dot{m} C_p \Delta T$$

where $\dot{Q}$ is the heat transfer rate, $\dot{m}$ is the mass flow rate, C_p is the specific heat and ΔT is the temperature rise of the air, a bearing power loss estimate of 0.16 Hp (120 W) is realized for a 3.0 scfm (0.10 kg/min) air flow assuming a temperature of 70°F (294 K) for the incoming air, and a maximum temperature of 200°F (366 K) for the discharged air.

VII. CONCLUSIONS

Deep groove and angular contact 25 and 30mm ball bearings were tested at high speeds using air-oil mist lubrication. Test results based on bearing outer race temperature indicate that with adequate oil and cooling air flow rates, stable bearing operation from 1.2×10^6 DN to 1.9×10^6 DN can be achieved, depending on the bearing. A cooling air flow rate of 1.5 scfm (0.05 kg/min) was judged not adequate for high speed bearing operation while flow rates of 3.0 to 6.0 scfm (0.10 to 0.20 kg/min) were judged adequate for the tested conditions of 50, 75, and 100 pounds (222, 334 and 445 N) thrust loads and a 25 pound (111 N) radial load.

Temperature variation with cooling air flow rate indicates that substantial increases in cooling air flow above an estimated 6.0 to 9.0 scfm (0.30 to 0.30 kg/min) may yield only slight improvement in extending the maximum bearing operating speed. An oil flow rate of 1.4×10^{-5} to 3.1×10^{-5} gal/min (0.05 to 0.12 mℓ/min) was apparently adequate for high speed operation, but no tests were conducted in which the oil flow rate was varied independently of the cooling air flow rate.

The deep groove bearings performed better at high speeds than the angular contact bearings in these tests, but this should be confirmed in subsequent testing. Under the established test constraints, maximum DN values of 1.9×10^6, 1.5×10^6, 1.4×10^6 and 1.26×10^6 were achieved on the 30mm deep groove, the 25mm deep groove, the 25mm angular contact, and the 30mm angular contact bearings, respectively.

VIII. RECOMMENDATIONS

The major effort during development of the test rig was design and fabrication of a reliable turbine drive unit. The bearing test unit was adapted from a previous project, and was not particularly suited to the present research. For any future testing, strong consideration should be given to the design and fabrication of a new test unit. Some recommended design features of the new unit are given below:

1) Wider support bearing spacing relative to the overhung shaft length.
2) Larger support bearings, perhaps 20mm.
3) Soft mount support bearings on elastomeric "0"-rings for improved damping.
4) Adjustable support bearing preload.
5) Enclosed housing to reduce support bearing oil mist loss.
6) Vibration and bearing temperature monitors.
7) Reliable speed transducer with direct readout.

The existing 25 and 30mm overhung test bearing housings could be used, and of course the new unit should couple to the existing drive turbine. The test bearing torque measuring system could be made operational by using a load cell with direct readout, and accelerometers should be installed on the overhung housing to monitor test bearing vibration. It is believed that the close support bearing spacing was the chief cause of many of the vibration problems encountered during testing.

With an improved test rig, the results presented should be confirmed to determine if the test rig characteristics had any significant influence. In particular, much better performance for the angular contact bearings was expected. Confirmation that the deep groove bearings are in fact more suitable for high speed use would be significant since angular contact bearings are typically used in high speed applications.

In future tests, a lubricant more suitable for high temperature use might allow higher speeds to be achieved. Any lubricant used, however, should be tested to insure that it atomizes properly in the air-oil mist generators. These tests are usually performed by the oil-mist generator manufacturer or supplier at little or no cost. Generally, data on a number of lubricants already tested is available from these sources.

The cage resonance observed for the 25mm deep groove bearing may have caused the temperature to rise sharply at approximately 55,000 RPM. Future work might be directed at the calculation of such cage resonances. Such an analysis may lead to better bearing selection or better cage design.

A final recommendation is in the area of statistical analysis. Future tests could potentially be more fruitful with preliminary and ongoing assistance from a statistician. With properly designed test procedures, the number of test runs required can be reduced and better prediction models can be realized.

REFERENCES

1. Parker, R. J., "Lubrication of Rolling Element Bearings," Bearing Design-Historical Aspects, Present Technology and Future Problems, Published by ASME 1980, pp. 87-110.

2. Bailey, J. I., and Galbato, A. T., "Evaluating Bearings for High-Speed Operations," Machine Design, October 8, 1981, pp. 141-146.

3. Palmgren, Arvid, Ball and Roller Bearings Engineering, S. H. Burbank and Co., Philadelphia 1945, p. 109.

4. Zaretsky, Erwin V., "Advances In High Speed Rolling Element Bearings," NASA TM 82910, 1982.

5. Schuller, Frederick T., and Signer, Hans R., "Performance of Jet- and Inner-Ring-Lubricated 35-Millimeter-Bore Ball Bearings Operating to 2.5 Million DN," NASA TP 1808, 1981.

6. "Design Manual for Lubrication," C. A. Norgren Co., Publication NT-1f, September 1981.

7. Hamrock, Bernard J., and Dowson, Duncan, Ball Bearing Lubrication the Elastohydrodynamics of Elliptical Contacts, John Wiley and Sons, New York, 1981, pp. 104-105 and p. 119.

8. Pinel, Stanley I., and Signer, Hans R., "Development of a High Speed, Small Bore Bearing Test Machine," NASA CR 135083, 1976.

9. Schuller, Frederick T., Pinel, Stanley I., and Signer, Hans R., "Operating Characteristics of a High-Speed, Jet-Lubricated 35-Millimeter-Bore Ball Bearing with a Single-Outer-Land-Guided Cage," NASA TP 1657, 1980.

10. Miyakawa, Y., Seki, K., and Yokoyama, M., "Study on the Performance of Ball Bearings at High DN Values," NASA TT F-15, 017, September, 1973.

11. Miyakawa, Yukio, Seki, Katsumi and Nomizo, Kunio, "Performance of Ball Bearings with Oil Mist and Jet Lubrication at High DN Values," Japanese National Aerospace Laboratory, 1977.

12. Rosenlieb, J. W., "Emergency and Microfog Lubrication and Cooling of Bearings for Army Helicopters," NASA CR 135195, 1978.

13. "Barden Precision Spindle and Turbine Ball Bearings," Barden Corporation, Catalog ST2, 1980.

14. Montgomery, Douglas C., and Peck, Elizabeth A., Introduction to Linear Regression Analysis, John Wiley and Sons, New York, 1982, p. 1, pp. 109-111, 293.

15. SAS Macro, VPI&SU Statistics Department Computer Program.

APPENDIX A: Test Rig Campbell Diagrams

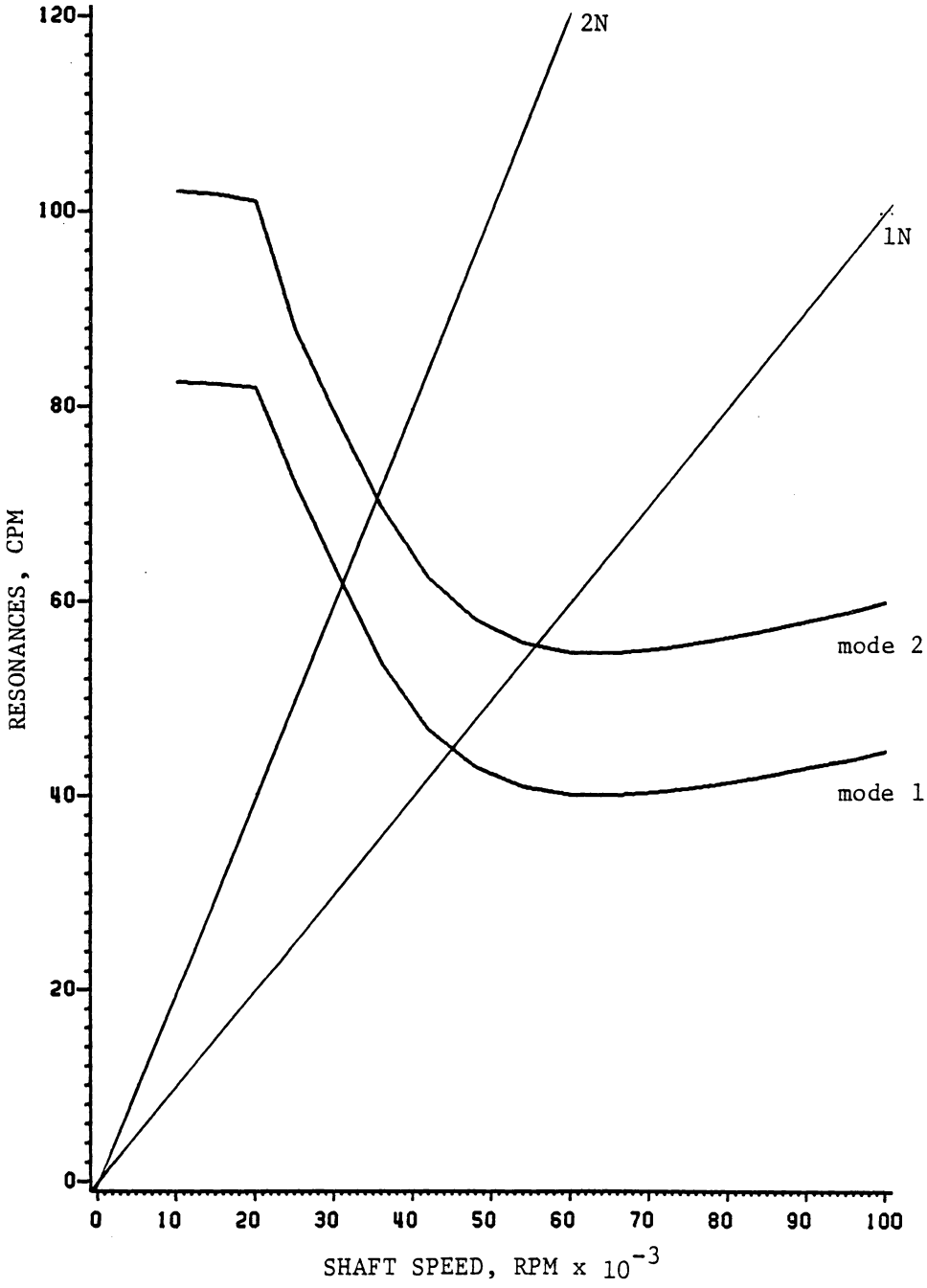

Fig. A-1. Campbell Diagram for the Drive Turbine

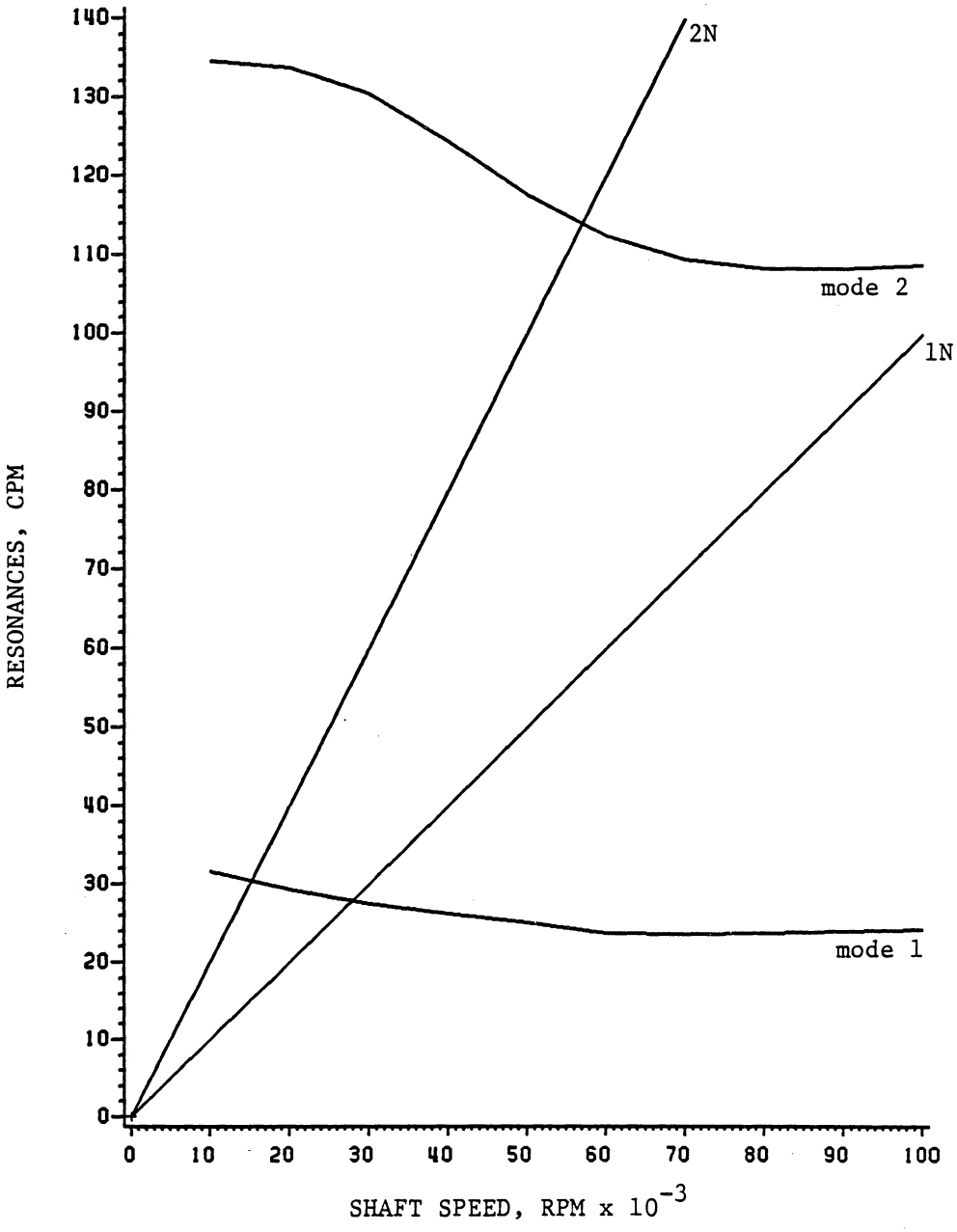

Fig. A-2. Campbell Diagram for the Bearing Test Unit with a 50 lb Test Bearing Thrust Load.

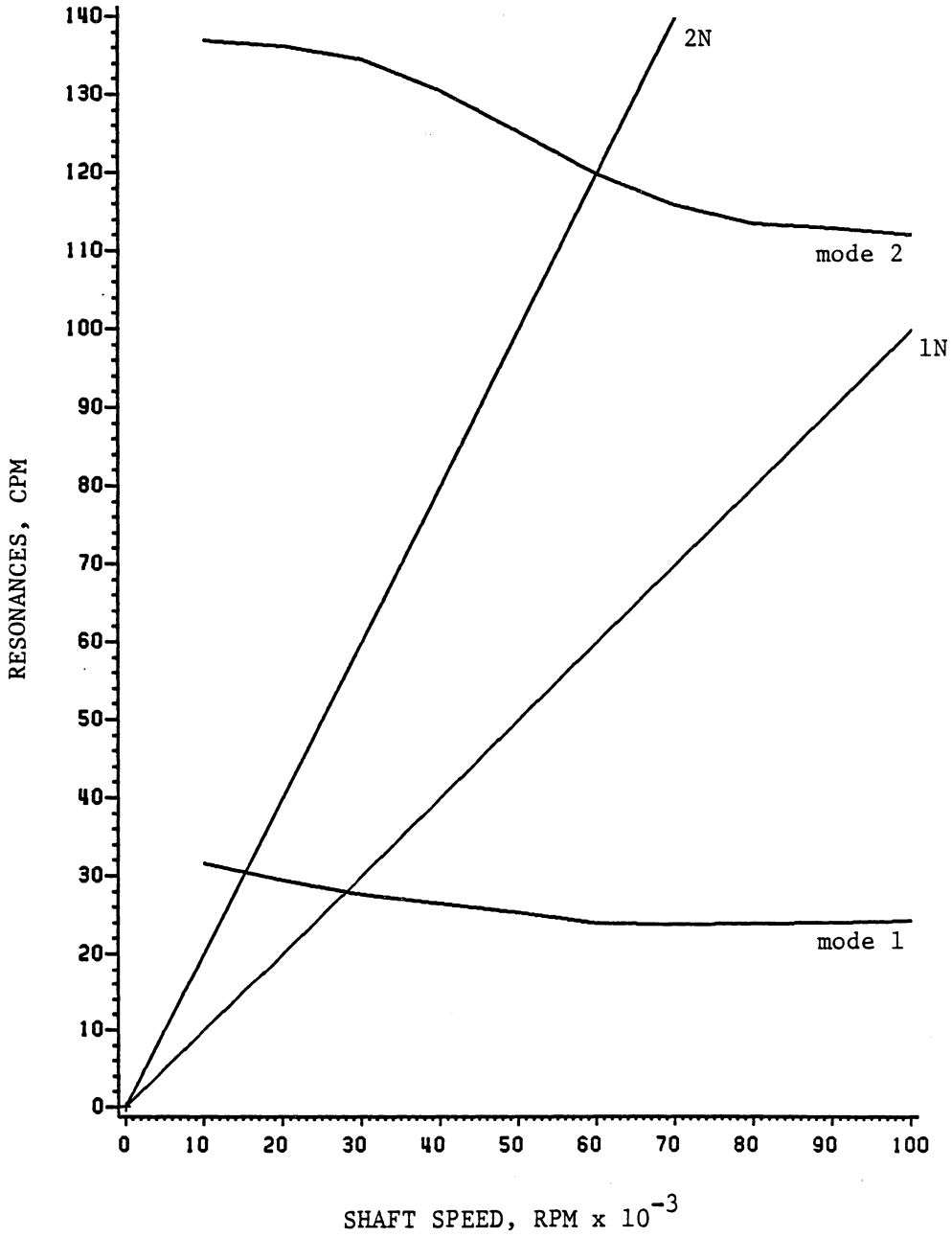

Fig. A-3. Campbell Diagram for the Bearing Test Unit with a 75 lb Test Bearing Thrust Load.

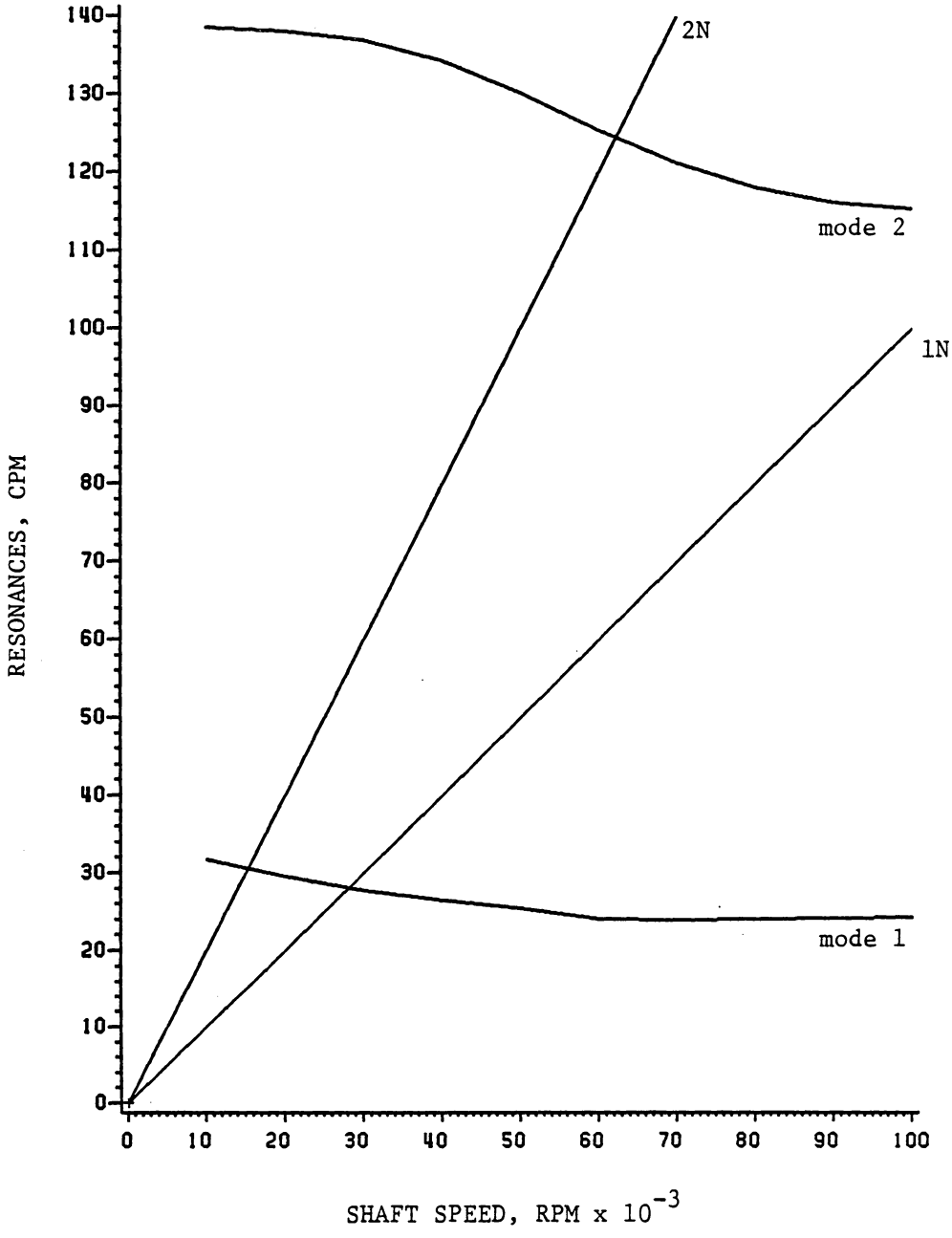

Fig. A-4. Campbell Diagram for the Bearing Test Unit with a 100 lb Test Bearing Thrust Load.

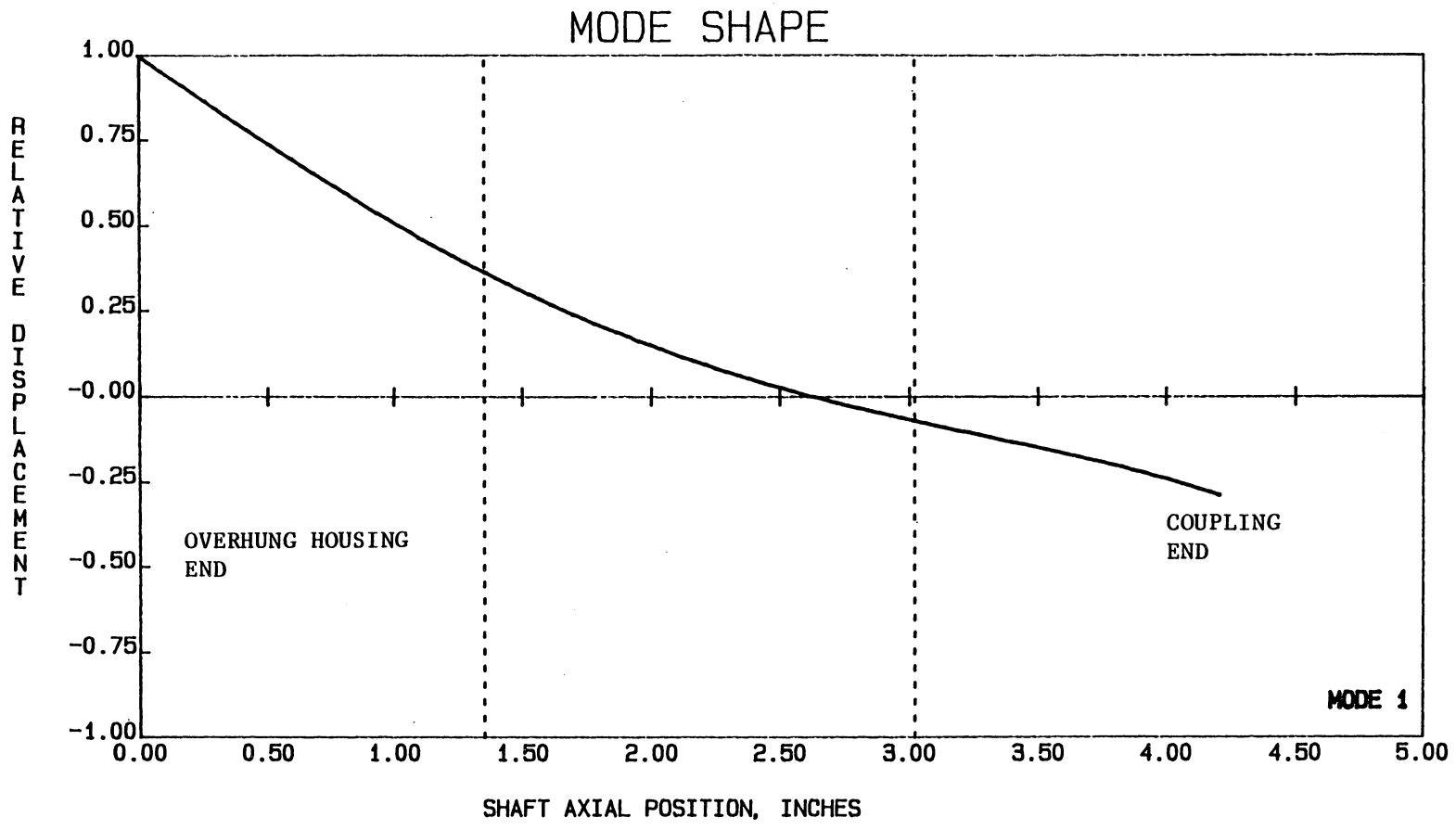

Fig. A-5. Bearing Test Unit Mode Shape

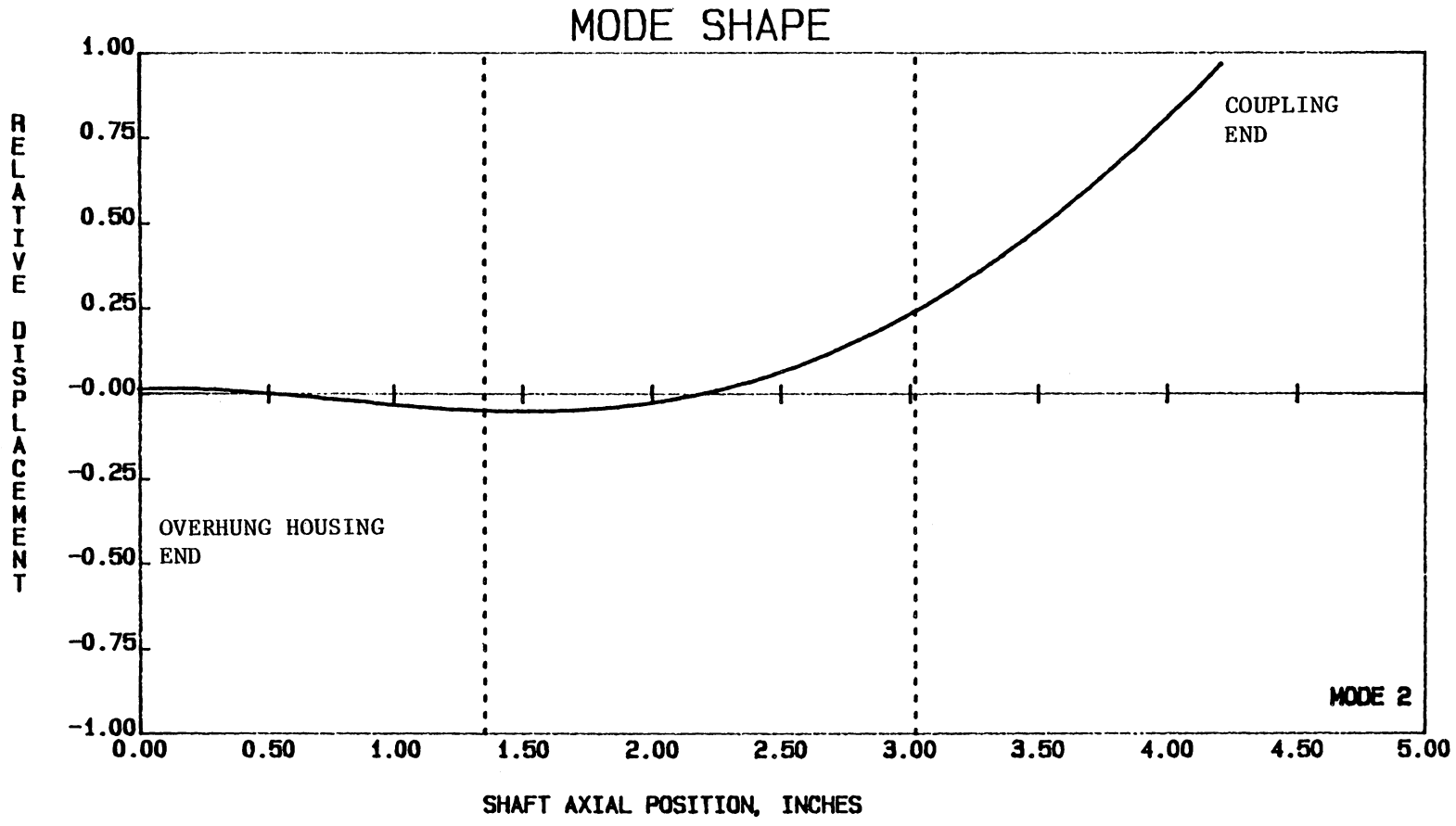

Fig. A-6. Bearing Test Unit Mode Shape

APPENDIX B: Regression Analysis Statistics

Table B-1. Regression Analysis Statistics for the 25mm Bearings

25mm Deep Groove Bearing (60,000 RPM maximum)

Variable	Coefficient, β	Standard Error	Variance Inflation
DN	0.150068	0.028255	64.55
DN^2	-2.79274×10^{-3}	1.314944×10^{-3}	480.19
DN^3	3.357571×10^{-5}	1.553963×10^{-5}	220.21
AF	-11.938175	2.435525	7.81
OF	341.986	130.866	7.29
L	0.269932	0.057210	0.49

25mm Angular Contact Bearing (56,000 RPM maximum)

Variable	Coefficient, β	Standard Error	Variance Inflation
DN	0.082463	0.012546	535
DN^2	0.0	-----	---
DN^3	8.37251×10^{-6}	4.68507×10^{-6}	6.64
AF	-23.775442	3.9753	8.58
OF	1034.665	119.977	7.29
L	0.126457	0.080251	0.45

Table B-2. Regression Analysis Statistics for the 30mm Bearings

30mm Deep Groove Bearing (63,000 RPM maximum)

Variable	Coefficient, β	Standard Error	Variance Inflation
DN	0.134735	0.010985	7.59
DN^2	-5.90795×10^{-4}	2.102232×10^{-4}	8.66
DN^3	0.0	----	----
AF	-24.505097	3.039199	8.57
OF	939.625	153.315	7.58
L	0.245667	0.061680	0.44

30mm Angular Contact Bearing (40,000 RPM maximum)

Varible	Coefficient, β	Standard Error	Variance Inflation
DN	0.092455	0.052367	78.52
DN^2	6.484516×10^{-3}	3.646543×10^{-3}	532.48
DN^3	-1.36658×10^{-4}	5.955264×10^{-5}	235.75
AF	-10.666424	3.16145	8.71
OF	247.838	162.864	7.51
L	0.246230	0.06797	0.46

The vita has been removed from the scanned document